ALL SELENIUM CONTAINING MACROCYCLES AND THEIR METAL COMPLEXES: SOME NOTEWORTHY RESULTS

Abstract

Researchers envisioned an analogous growth of the related macrocyclic polyselena ethers after the discovery of sulphur coronands as well as its extensive yet fascinating coordination chemistry. Selena-macrocycle productions as well as their coordination chemistry investigations have gathered a lot of interest following an accidental discovery of selena-crown ethers. The development and production of novel homo along with mixed donor selenoethermacrocyclic molecules have received a lot of attention lately in order to investigate potential binding behaviours against transition and non-transition metal ions. The majority of research on Se-macrocycles has been investigative synthetic studies to understand the nature of their coordination chemistry. In this chapter, coronand-macrocycles having all selenium donor atoms have been discussed, from their synthesis to their metal complexation along with description of several crystal structures. In addition, selenocyclophanes have also been also been briefly included.

Author

Partha Pratim Das
P. G. Department of Chemistry
Magadh University
Bodh-Gaya, Bihar, India.

I. INTRODUCTION

The potential of synthesized macrocyclic ligands to serve as selective metal-ion binding substances has been extensively studied. The cyclical structure of macrocycles, that offers a "preformed" receptor cavity providing the metal interaction spot, allows them to be appropriate for this purpose. Invention of macrocycles having extremely sensitive sensors towards metal cations has continued following the landmark findings of Pedersen[1], Lehn[2], and Cram[3], that entailed the synthesis of cation selective crown ethers, cryptands, as well as spherands. Numerous studies have been done on the prospect of macrocyclic compounds to serve as selective metal-ion interacting substances. Macrocycles are well suited for this purpose due to their cyclic framework, which features a built-in receptor pocket which serves as the metal attaching point. Depending on the volume inside the macrocycle's cavity, the restricted conformational adaptability of the macrocyclic ring allows it to adjust to the steric (as well as electrical) requirements of the metal ions. Macrocycles have a variety of applications, mainly related to the sensing and separation of various substances. The utilization of macrocyclic ligand molecules as trustworthy components enabling the development of supramolecular frameworks is a result of what is known as the macrocycle effect that happens whenever these substances surpass its open-chain equivalents in regards to kinetic and thermodynamic stability. There are several macrocycles reported in literature that contain exclusively oxygen and sulfur as donor atoms or a mixture of oxygen, sulfur and nitrogen donor atoms. A lesser amount of study has been done about their third and fourth group companions, Selenium as well as Tellurium containing macrocyles. When the larger Se is included, the macrocycle cavity enlarges, allowing a number of novel coordination behaviors. Selenium's greater potential for σ-donating also facilitates the association of several metal ions, in addition. Numerous d- and p-block components were demonstrated to display extensive coordination chemistry for polyselenoether macrocycles. Macrocycles with selenium as well as sulfur, oxygen, nitrogen, phosphorus donor atoms are also hugely reported in literature. Considering these may combine multiple metals having various characteristics as well as oxidation states within just one cavity, macrocycles containing mixed hard as well as soft donors became increasingly important as time passed. However, this chapter exclusively discusses the chemistry for macrocyclic ligands that contain only selenium donor sites. Additionally, ^{77}Se NMR offers a technique for investigating configurations in solutions that wasn't available with the smaller derivatives oxygen and sulfur.

II. SELENOCYCLOPHANES

First selenacyclophanes[4] are described as 2,11-diselena[3,3]metacyclophane [L^1], 2,11,19-triselena[3,3,3]metacyclophane [L^2], and the related dimethyl [L^3] and trimethyl counterparts [L^4]. These were made via combining xylene bromide with sodium selenide, although in low yield [Scheme 1]. The reaction of the dibromide with the extremely air-sensitive intermediary substances diselenol or its dianion in an alkaline atmosphere produces a diselenide-polymer that is hard to separate in addition to the intended coupled product, which accounts for the small amount produced of the products. A method that offers significantly greater yields of selenacyclophanes than the sodium selenide coupling was proposed[5] [Scheme 2]. Through the reductive coupling of bisselenocyanates and dihalide, several cyclic diselenides, including L^1, alicyclic diselenides, and diselenacrown ethers, were produced. Additionally, because no unwanted polymer is formed, this novel approach makes

it simple to create both symmetrical and asymmetrical diselenacyclophanes. It also makes it simpler to purify the end products. Later, using the (π-benzene)Ru^{II} moiety, the coordination chemistry of 2,11-diselena[3,3]orthocyclophane was investigated[6]. Cyclophane bonds as bidentate Se donors in [(η^6-C_6H_6)Ru(Selenocyclophane)X]X [X = Cl or Br].

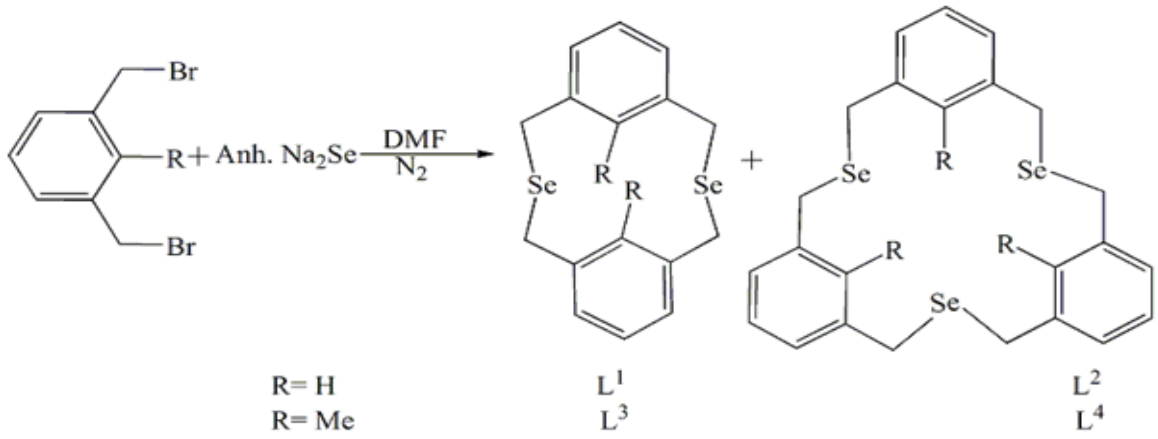

Scheme 1

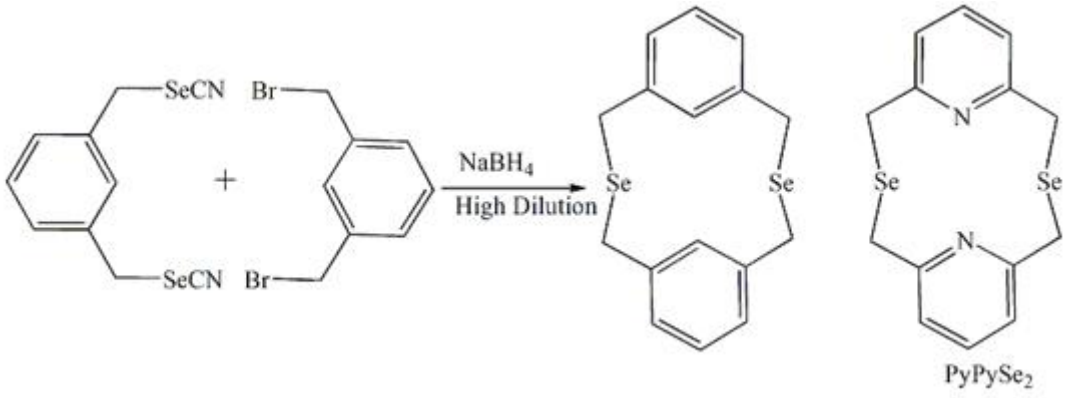

Scheme 2

The formation of 2,11-diselena[3,3] (2,6) pyridinophane ($PyPySe_2$) was reported by researchers. The most common configuration of $PyPySe_2$ is *syn*-, which involves twisting the methylene bridges and flipping the pyridine rings[7].The equivalent adaption of both metal ions in the heterophane cavity is indicated by identical stability constants for Ni^{2+} and Cu^{2+} compounds with $PyPySe_2$.The values of the stability constant also suggest a usual host-guest relationship. Contrary to the Ni^{2+} compound of the thia counterpart, in which the heterophane is distorted from the syn configuration, the framework of $[Ni(PyPySe_2)(H_2O)_2][ClO_4]_2$ (Figure 1) displays an extremely symmetric heterophane in a *syn*- configuration.

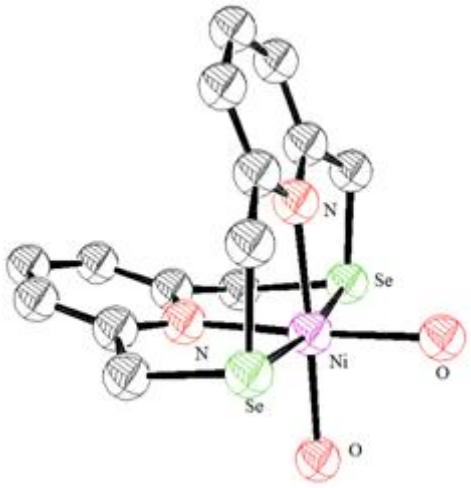

Figure 1

When the linked H_2O was substituted by chloride, intriguing variations in the spectroscopic and conductivity characteristics of the Cu^{II} compound were found. At normal temperature, the heterophane and the metal and charge-transfer compounds it contains act as semiconductors, with the $[Cu(PyPySe_2)Cl_2]$ complex displaying the best conductivity[8]. The complexation and conductivity characteristics of selenacyclophanes were never reported before.

III. SELENIUM MACROCYCLICPOLYETHERS

While thiacrown ethers tend to coordinate with transition metal ions, crown ethers can form compounds with Group I and Group II metal ions. Passion at selenium coronands developed following the unintentional discovery of macrocyclic polyselenoethers via the combination of sodium propane-1,3-bis(selenolate) in liquid NH_3 and Tetrahydrofuran with dibromoethane. Lighter sulfur counterparts have configurations that are drastically distinct compared to those of their oxygen equivalents and produce complexes of metals with unexpected electronic compositions and redox characteristics. The generation of selenacrown ethers made it possible to create novel compounds. Numerous groups worldwide have looked into different metal compounds of selenacrown ethers.

1. **Synthesis of Ligands:** L^5–L^{12} are the first illustration of a novel class of selenium coronands[9,10,11]. Their schematic synthesis is shown in scheme 3. In the crystalline state of 1,3,7,9-tetraselenocyclododecane (L^5), Se inhabit alternative corners and lateral spots in two different quadrangular configurations[9].Contrarily, in solution, the favorable shape of L^5 and its 5,5,11,11-tetramethyl counterpart (L^7) is a [3333] quadrangle that has Se holding just side sites[10].Although not ultimate, the molecular framework for L^9 includes two ordered and one disordered molecules. Both types of molecules are [3535] quadrangles containing Se atoms arranged alternately in corner and side spots along the long edges[11]. There is only one conformer with crystallographic inversion symmetry in the crystalline form of L^{10}. Although not quadrangular, it is possible to picture the molecule as having developed through the compression of a [4848] quadrangle[11]. One conformer is found for L^{12}, and it is positioned on an inversion center in the crystal

structure. Having Se atoms at each of its four corners, the molecule is a [3434] quadrangle. In the above arrangement, molecules are packed corner to corner, producing a strong Se.....Se interaction[11]. The figures are shown in Figure 2.

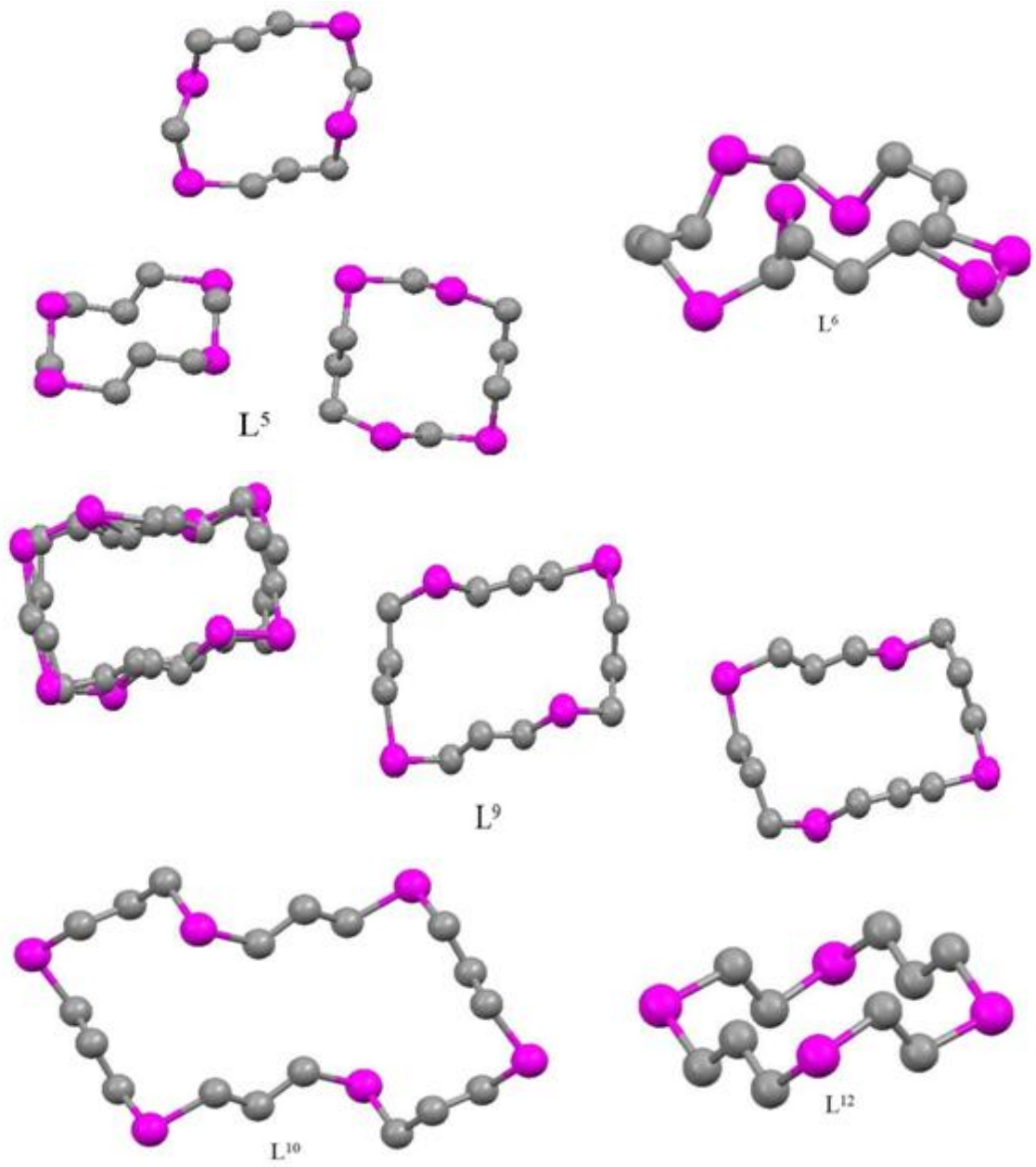

Figure 2

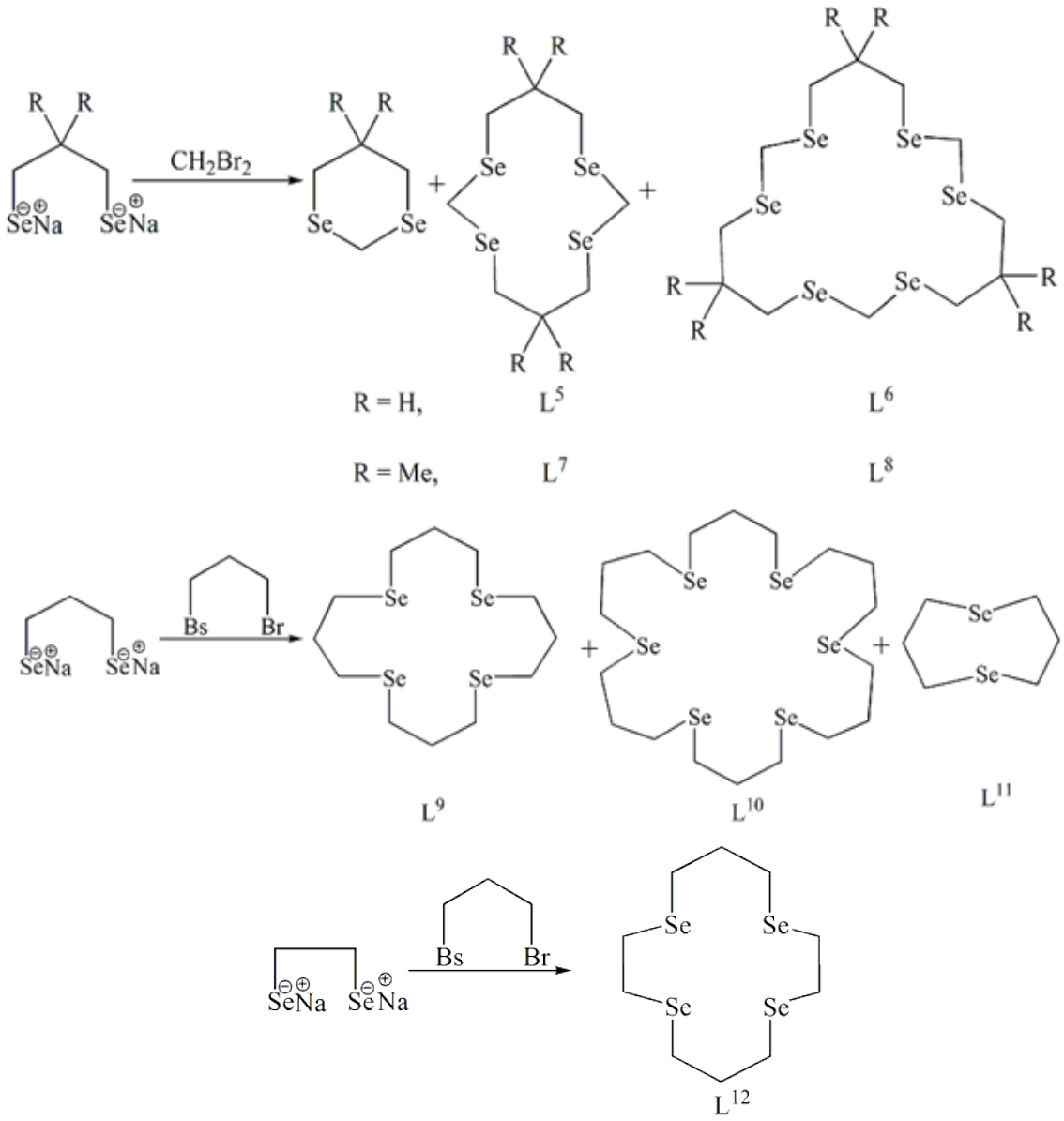

Scheme 3

The preparation of macrocycles with an even number of component Se atoms is perfectly suited to the aforementioned technique for the single-step production of Se coronands. The aforementioned laboratory published the first instances of the sequential production[12] of two novel Se coronands, L^{13} and L^{14}, which included an odd number of Se atoms and offered intriguing possibilities for additional research. The gauche C-Se-C-C bond torsion angles are multiplied by a factor of two in the molecular framework[13] of L^{13}. The synthetic routes are shown in Scheme 4. Figure 3 displays the crystal structure of L^{13}.

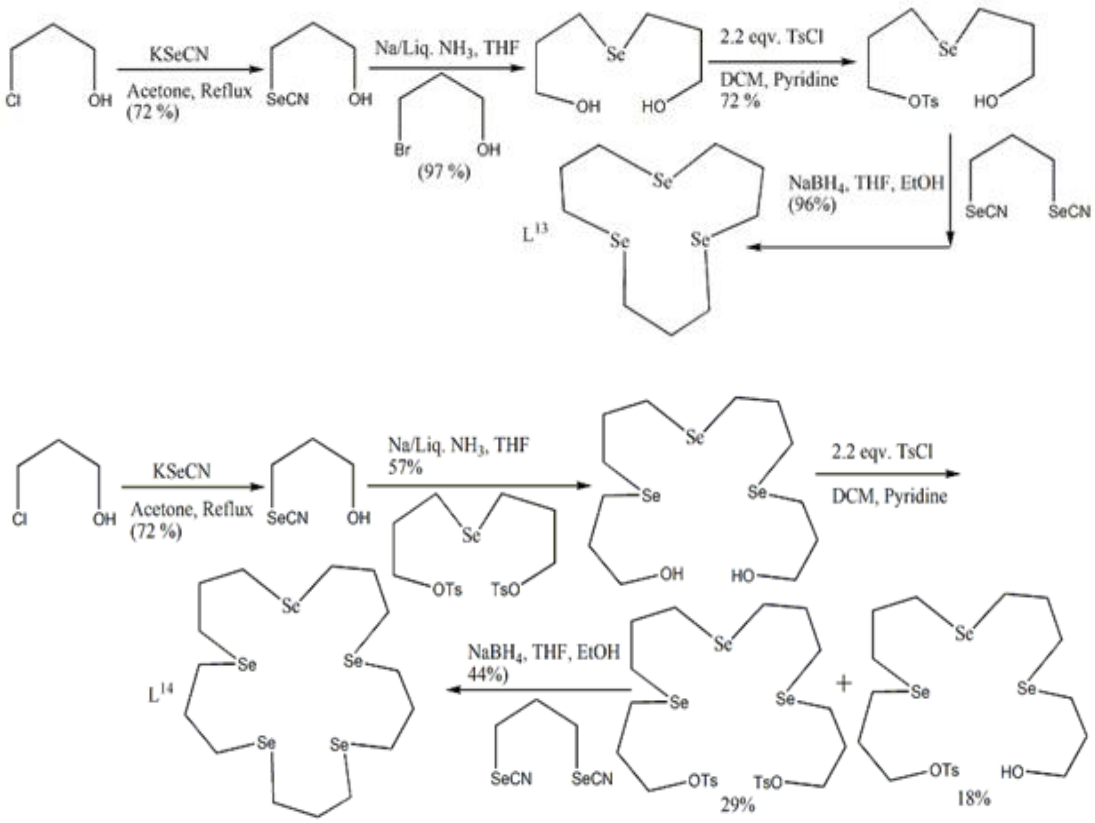

Scheme 4

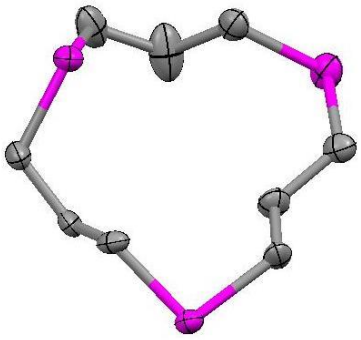

Figure 3

In order to produce functionalized Se coronands to incorporate into polymers or to enable the simple linking of aliphatic or functionalized chains, the previously stated process was improved[14]. The aforementioned molecules are useful for creating membrane transport systems along with transition metal ion-selective electrodes, as well as for generating water-soluble or micellar transition metal ion transport systems. The appropriate hydroxyl-functionalized bis-selenocyanate molecule was used to produce the hydroxyl-functionalized di and tetra selenoether macrocycles L^{15}, L^{16}, and L^{17}. The synthetic procedures are shown in Scheme 5 and 6. Utilizing those hydroxy functionalized Se coronands, an additional functional group (acrylate ester) is then tethered to them to generate an active monomer, which is the approach for the production

of the polymeric Se coronands. These are the first electroactive Se coronands that are polymer attached. These are shown in scheme 7 and 8.

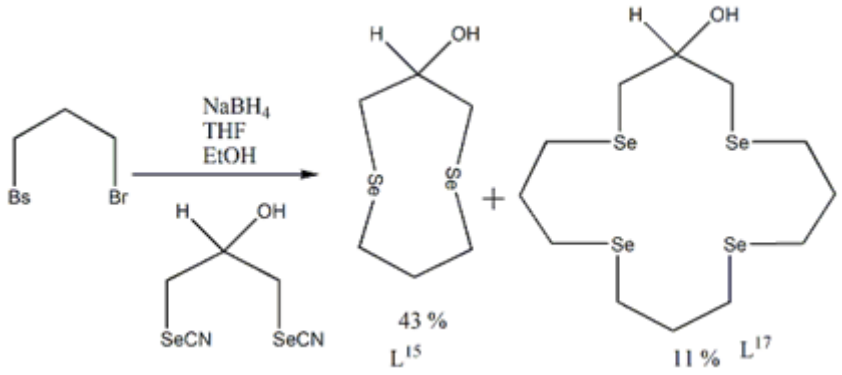

Scheme 5

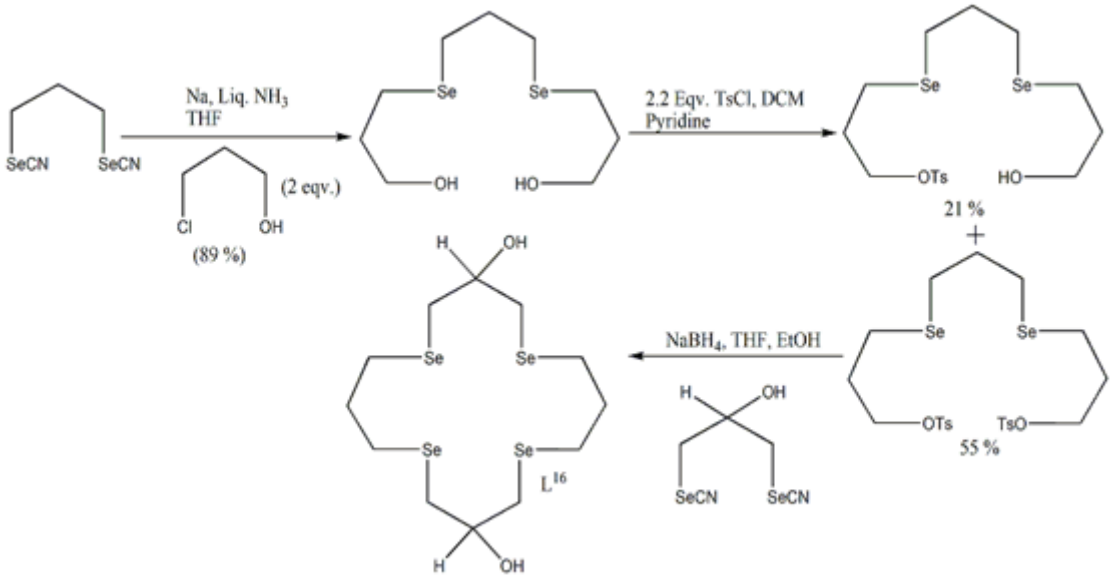

Scheme 6

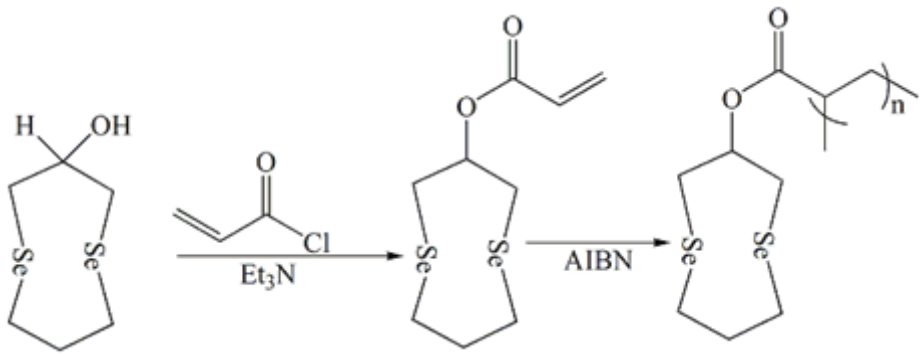

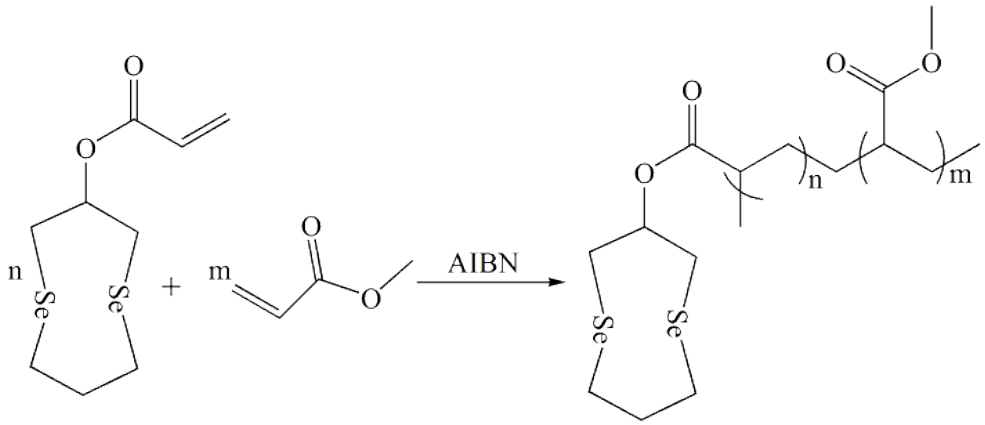

Scheme 7

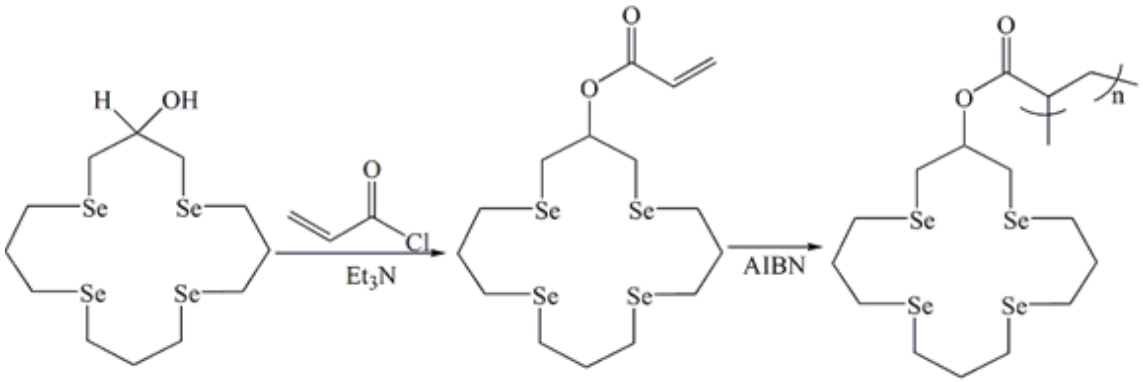

Scheme 8

According to Scheme 9, an entirely new Se coronand (L^{18}) was produced by stepwise reactions[13]. Two conformers are superimposed in a disorderly manner in the framework of L^{18}. The two arene rings of this coronand are almost coaxial, which is an intriguing characteristic (Figure 4). By reacting sodium 1,2-benzenediselenolate with 1,2-bis((3-halo-1-ethyl)-seleno)benzene, this synthetic method was extended for production of equivalent selenoether, with just two carbon bridges, but it was unsuccessful because of the generation of labile ethylene episelenonium ions that broke down by ethylene extrusion.

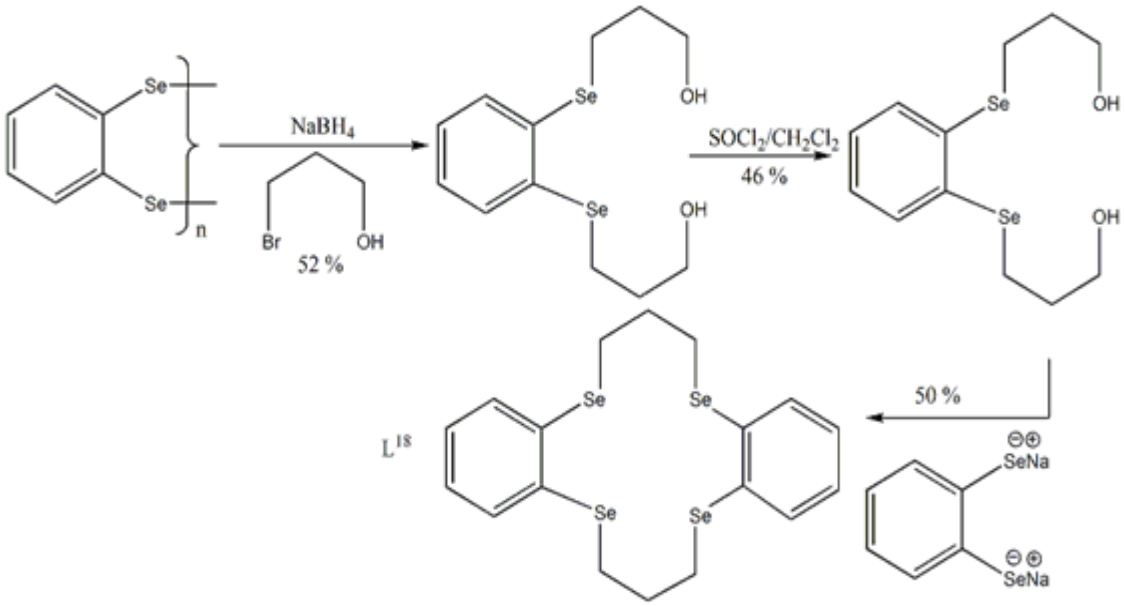

Scheme 9

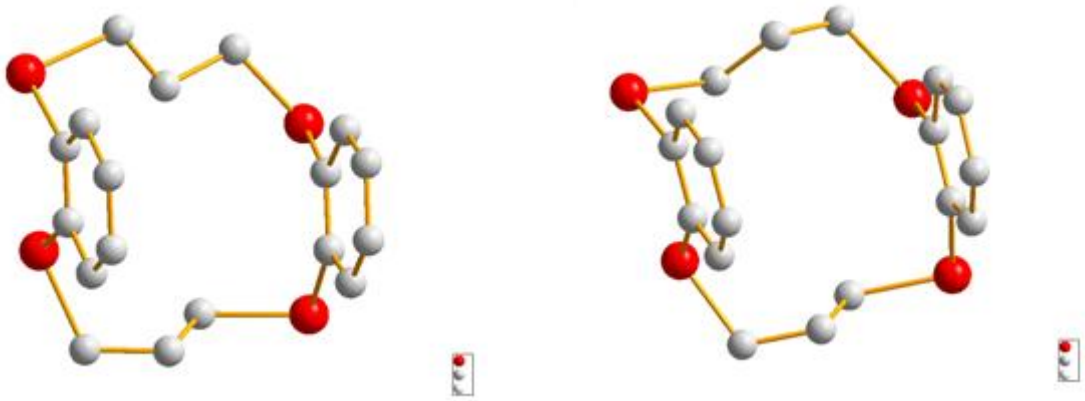

Figure 4

L^{19} was brand-new symmetric diselenoperi-bridged naphthalene[15]. The facile electrochemical oxidation of L^{19} and its interaction with concentrated sulfuric acid to produce selenoxide provide evidence for the presence of the peri-Se-Se connection. As shown in Scheme 10, fresh macrocyclicpolyselenides with naphthalene rings, L^{20}, L^{21}, and L^{22}, were produced[16,17] using the diselenide L^{19}. Tetraselenide L^{22}'s architecture reveals intra-molecular π–π stacking of the naphthalene rings and transannular Se…..Se interactions (Figure 5). The selenides L^{20}–L^{22}'s cyclic voltammograms exhibit reversible oxidation bands with exceptionally low oxidation potentials. The destabilization of macrocyclicpolyselenides by transannular lone pair-lone pair repulsion and stabilization of the oxidized products by peri selenium involvement, or the building of bonds among the two selenium atoms, are attributed to these simple oxidations of L^{20}–L^{22}. While L^{22} produced ring-contracted products, L^{20} and L^{21} hydrolyzed in concentrated sulfuric acid produced stabilized monoxides.

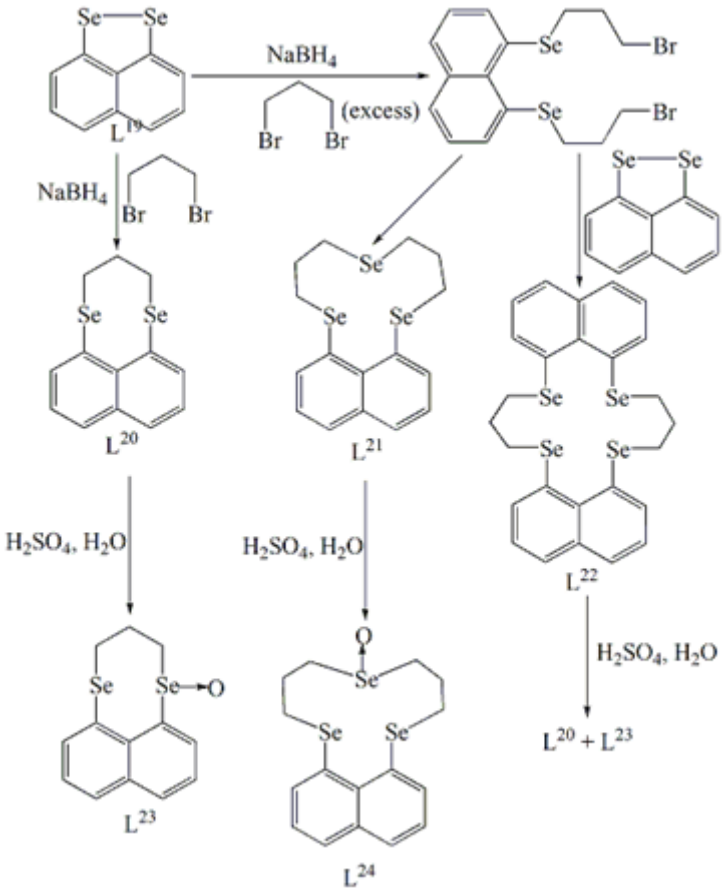

Scheme 10

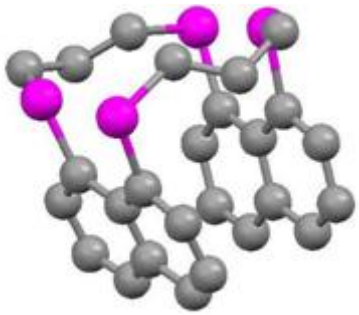

Figure 5

Scientists discovered a novel method to prepare polyselenoether macrocycles. Three novel polyselenoether macrocycles, L^{25}, L^{26}, and L^{27}[Figure 6], are produced as a result of the catalytic cyclo-oligomerization of 3,3-dimethylselenatane (Scheme 11)[18,19].The authors employed a method quite similar to this one in order to produce a variety of thioethermacrocycles. The macrocycles' gem-dimethyl groups are always pointed outward of the rings' surface. It's interesting to note that some methylene units are pointed inside the rings. The ring configurations and molecular packing

precisely resemble that of the previously described sulfur homologues[20]. The catalytic cycle is shown in Scheme 12.

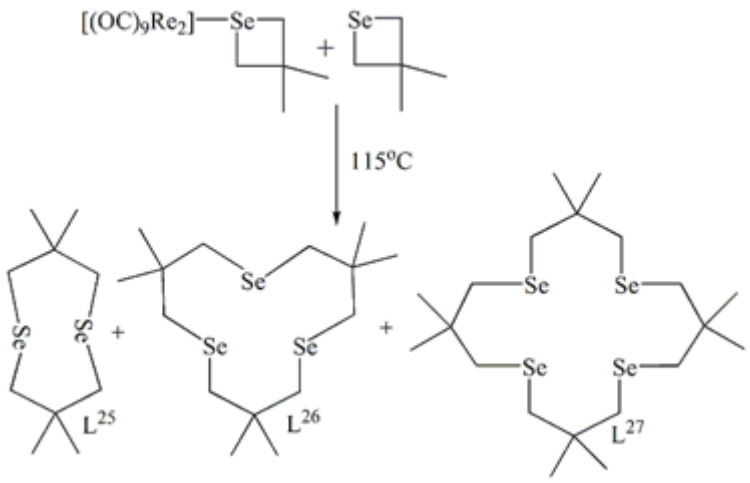

Scheme 11

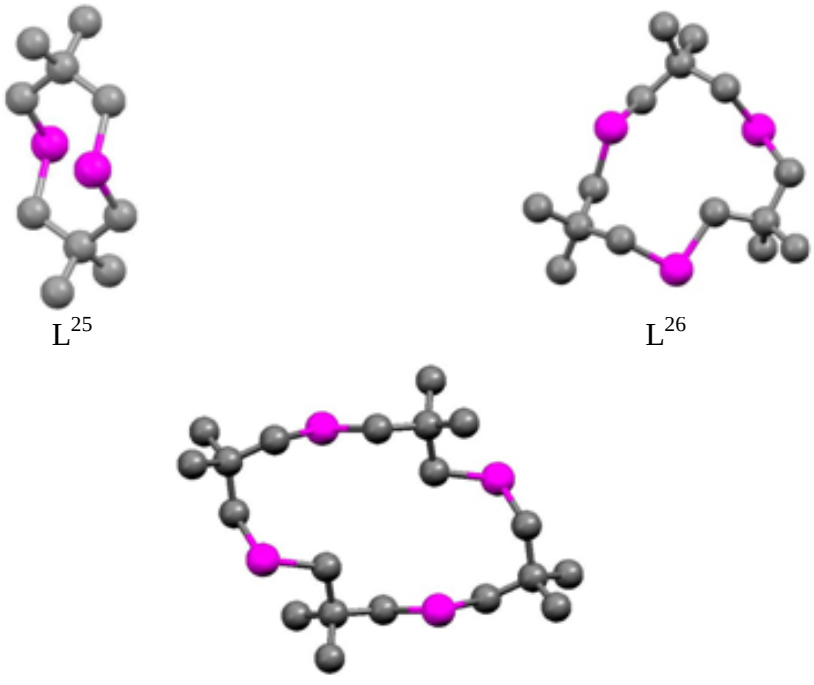

Figure 6

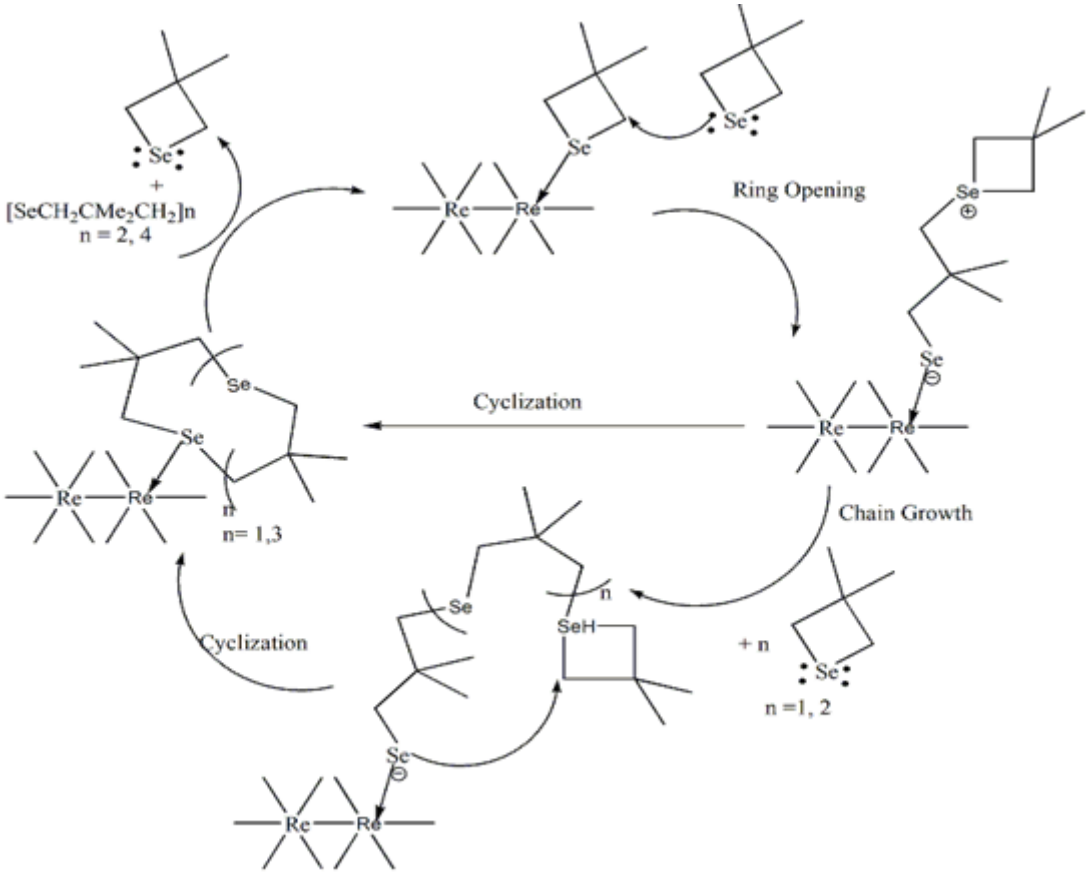

Scheme 12

It has been suggested that a [1+1] cyclization of $NCSe(CH_2)_3SeCN$ with o-$C_6H_4(CH_2Br)_2$ led to an easy production[21] of L^{28}. However, a combination of L^9, L^{10}, L^{11}, and higher polymers were produced by a similar reaction with $Br(CH_2)_3Br$. Se atom lone pairs can be seen protruding from the ring in the structure of L^{28} (Figure 7).These type of Se-crown ethers[22][Figure 8] have been employed as valuable and heavy metal ion extractors. In presence of Co^{II}, Ni^{II} etc., they are effective extractors for Cu^{I}, Pd^{II}, Hg^{I}, and $MeHg^{II}$. This Se-crown ethers act as better extractors towards $MeHg^{II}$ compared to the chemically comparable thia-crown ethers.

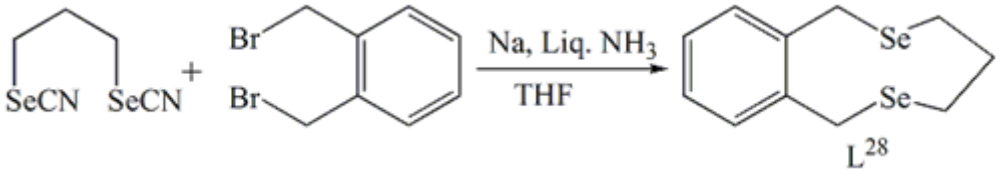

Scheme 13

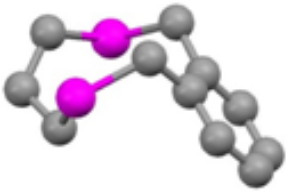

Figure 7

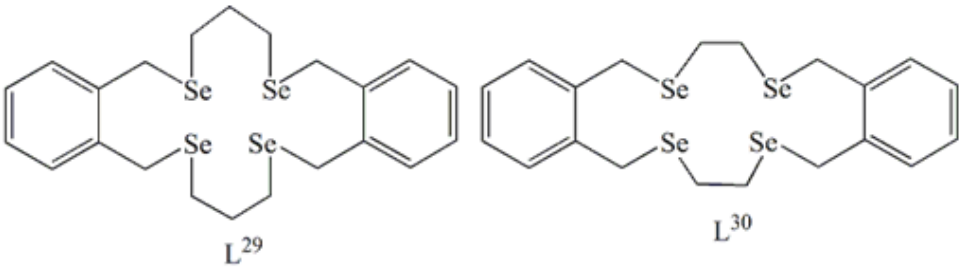

L^{29} L^{30}

Figure 8

2. Coordination Chemistry with Metal ions

- **With Transition Metal ions:** The early transition metals of the form $[M(CO)_4(L^{11})]$[23] (M= Cr, Mo, or W) ($[Cr(CO)_4(L^{11})]$, $[Mo(CO)_4((L^{11}))]$, $[W(CO)_4(L^{11})]$) *cis*-disubstituted tetracarbonyl entities has been identified. The L^{11} ligand fills two sequentially *cis*- coordination spaces in the framework of $[W(CO)_4(L^{11})]$, and the CO ligands complete the deformed octahedral shape. Figure 9 shows that the W-CO length *trans*- to Selenium is substantially smaller compared to the *trans*- to CO. Ligand stays in a chair-boat configuration. *fac*-Tricarbonyl compounds $[MX(CO)_3(L^{11})]$ (M=Mn or Re and X=Cl, Br or I) ($[MnCl(CO)_3(L^{11})]$, $[MnBr(CO)_3(L^{11})]$, $[MnI(CO)_3(L^{11})]$, $[ReCl(CO)_3(L^{11})]$, $[ReBr(CO)_3(L^{11})]$)[21]are also reported. The CO stretching frequencies are similar to those of the structurally related fac-acyclic diselenoether structures, suggesting that the L^{11} molecules have a fac-tricarbonyl configuration[24]. In contrast to similar acyclic diselenoether compounds, where many invertomers were present, just one invertomer was found in this compound. These compounds are isostructural, with the metal centers of each presenting a deformed octahedral configuration composed of three mutually *fac*-CO ligands, a bidentate L^{11}, and a halide. A chair-boat-like shape is adopted by the linked diselenoether. Synthetic routes of the complexes are shown in Scheme 14. Structures of $[MnBr(CO)_3(L^{11})]$, $[ReBr(CO)_3(L^{11})]$ and $[W(CO)_4(L^{11})]$ are shown in Figure 9.

$$[M(CO)_4(nbd)] + L^{11} \xrightarrow[\text{Reflux}\ N_2\ \text{atm}]{\text{Chloroform}} [M(CO)_4(L^{11})]$$

$$[MX(CO)_5] + L^{11} \xrightarrow[\text{Reflux}\ N_2\ \text{atm}]{\text{Chloroform}} [MX(CO)_3(L^{11})]$$

Scheme 14

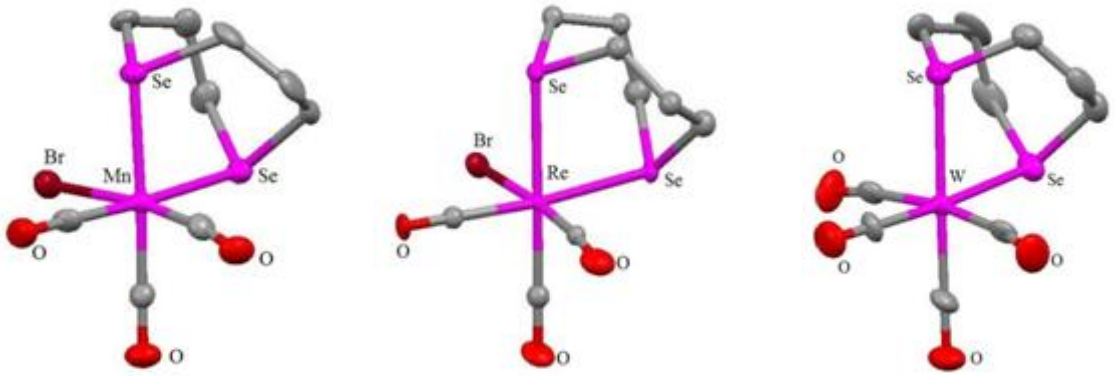

$[MnBr(CO)_3(L^{11})]$ $[ReBr(CO)_3(L^{11})]$ $[W(CO)_4(L^{11})]$

Figure 9

In solution, $[RuCl_2(L^{11})_2]$ maintains its cis-dichloro configuration[25]. It was not possible to transform *cis*-$[RuCl_2(L^{11})_2]$ into the *trans*- isomer. Although the yield was lower, treating $[RuCl_2(py)_4]$ with L^{11} results in $[RuCl_2(L^{11})_2]$ as a combination of *cis*- and *trans*- isomers. $[RhCl_2(L^{11})_2](BF_4)$ is also reported[26]. Scheme 15 shows the reactions involved.

$$[Ru(DMF)_6]Cl_3 + L^{11} \xrightarrow[\text{Reflux}\\ \text{4 hours}]{\text{EtOH}\\ N_2\ \text{Atm}} \text{cis-}\ [Ru(Cl)_2(L^{11})]$$

$$[\{Rh(CO)_2Cl_2\}_2] + L^{11} + HBF_4 \xrightarrow[\text{Reflux}\\ \text{30 min}]{\text{Acetone}} [RhCl_2(L^{11})_2](BF_4)$$

Scheme 15

The spectral analysis of $[M(L^{11})Cl_2]$ (M= Pd or Pt) and $[MMeSe(CH_2)_3SeMeCl_2]$[27], which are contemporaneous to *cis*-planar Se_2Cl_2 donating sets, are equivalent. The coordination of the two Selenium donors of the bidentate L^{11} ligand and the two *cis*-Cl ligands to the metal ion may be seen in the framework of $[Pd(L^{11})Cl_2]$ (Figure 10). The chair-boat configuration is adopted by the coupled L^{11} ligand. Complexes of the type $[M(L^{11})_2][PF_6]_2$ (M= Pd, Pt) are also reported[28]. ($[Pt(L^{11})C1_2]$, $[Pd(L^{11})Cl_2]$, $[Pt(L^{11})_2]$ $[PF_6]$, $[Pd(L^{11})_2][PF_6]_2$; Scheme 16) Enantiomers are not possible because of the linked cyclic ligands' high degree of symmetry. As opposed to this, acyclic diselenoether complexes have meso and DL enantiomers[29].

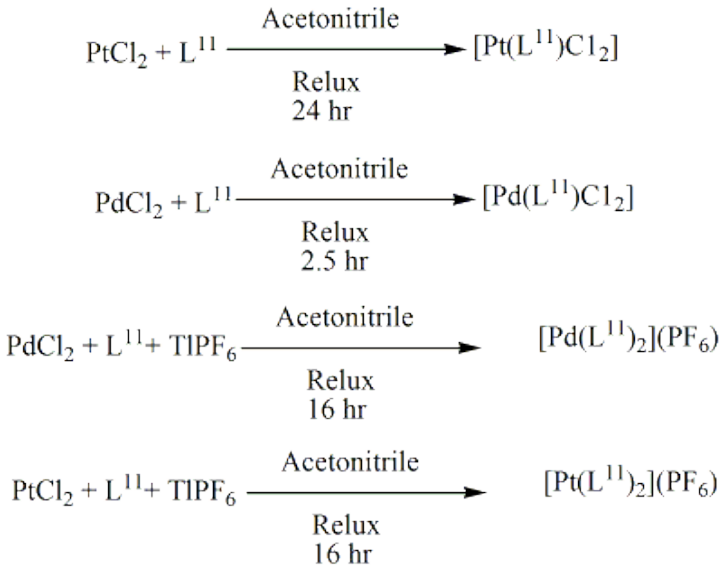

Scheme 16

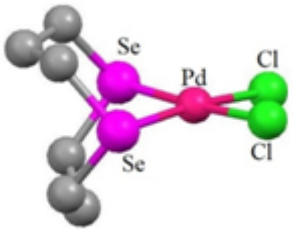

$[Pd(L^{11})Cl_2]$

Figure 10

Interaction of $[PtMe_2(SMe_2)_2]$ and L^{11} led to the formation of the planar $[PtMe_2(L^{11})]$ compound. Owing to the L^{11} ligand's cyclic nature, which rules out the prospect of stereoisomers, just one form of the compound is observable. In excellent yield, the deformed octahedral compound $[PtMe_3I(L^{11})]$ being synthesized. This is the first instance of a cyclic Se-ether linkage in an alkyl Pt^{IV} compound[29].

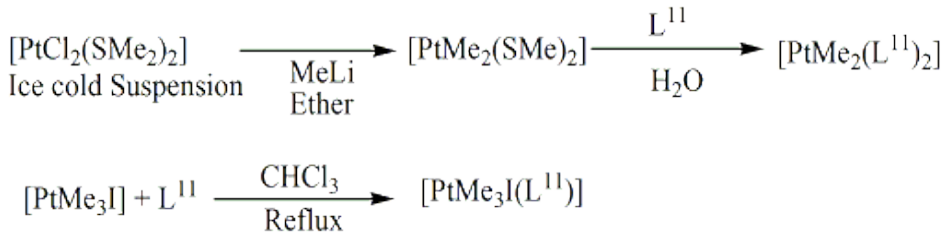

Scheme 17

Compounds of kind $[(AuCl)_2(L^{11})]$ and $[(M(L^{11})_2]Y$ (M = Cu, Y = PF_6; M = Ag, Y = BF_4) were published by researchers[21] ($[Cu(L^{11})2]PF_6$, $[Ag(L^{11})_2]BF_4$ [Figure

11] and $[(AuCl)_2(L^{11})]$). The distorted tetrahedral Ag^I monomer and two bidentate L^{11} ligands are visible in the crystal form of the Ag^I compound. The polymeric architecture of the Ag^I compound of acyclic di-Se-ether, $[Ag_n\{PhSe(CH_2)_3SePh\}_{2n}]^{n+}$, differs from the discrete molecular framework of this compound. Contrary to the chair-boat shape for all previous structurally characterized L^{11} compounds, the L^{11} ligands assume a boat-boat configuration. When L^{11} binds to Ag^I in a bis(bidentate) way, it takes on a boat-boat shape. However, when it attaches to the metal ions Pd(II), W(0), and Mn(I) in a bidentate fashion, a chair-boat conformation is seen.

$$L^{11} + [Cu(MeCN)_4](PF_6)] \xrightarrow[RT]{\text{Acetone}} [Cu(L^{11})_2](PF_6)$$

$$L^{11} + AgBF_4 \xrightarrow[RT]{\text{Acetone}} [Ag(L^{11})_2]BF_4$$

$$L^{11} + [AgCl(tht)] \xrightarrow[0^oC]{\text{Acetonitrile}} [Ag(L^{11})_2]BF_4$$

Scheme 18

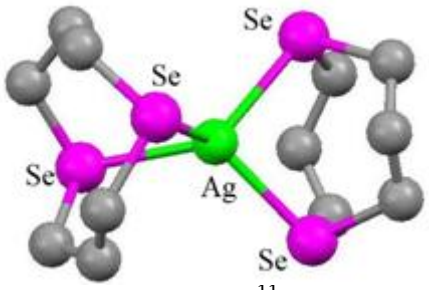

Cation of $[Ag(L^{11})_2]BF_4$

Figure 11

Blue, moisture-sensitive Cr^{III} complex $[CrX_2(L_9)](PF_6)$ has been published[30]. The failure of efforts to produce comparable compounds using the ligand L^{11} reflects the diselenoether's inferior coordinating ability to that of L^9. Researchers outlined how to synthesize the seven-coordinate M^{II} entity $[MX_2(CO)_3(L^9)]$ (M=Mo or W and X=Br or I)[23]. Complete characterization was not accomplished due to these compounds' low solubility in chlorocarbons and breakdown in coordinating solvents. The seven-coordinate structure with bridging L^9 indicated by comparing the IR data of the dinuclear complexes with an equivalent seven-coordinate thioether macrocyclic derivative, can be expressed as $[Mo_2X_4(CO)_6(\mu\text{-}L^9\text{-}Se,Se',Se'',Se''')]$. The W^{II} combination of L^9, in contrast, has a mononuclear structure with two Selenium donors and two non-coordinated Selenium atoms.In the mononuclear compound $[ReCl(CO)_3(L^9)]$ as well as the dinuclear compound $[\{MnCl(CO)_3\}_2(L^9)]$, L^9 functions as a bidentate ligand, freeing up two Selenium donor atoms for use in subsequent reactions. There have also been reports of the vivid orange cationic

Mn^{I} compound *fac*-$[Mn(CO)_3(\eta^3\text{-}L^9)](CF_3SO_3)$[23]. All the reactions are shown in Scheme 19.

$$[CrX_3(thf)_3] + TlPF_6 + L^9 \xrightarrow[N_2]{MeNO_2} [CrX_2(L^9)](PF_6) \quad X = Cl/Br$$

$$[\{MoBr_2(CO)_4\}_2] + L^9 \xrightarrow[RT]{CHCl_3} [MoBr_2(CO)_3(L^9)]$$

$$[\{MoI_2(CO)_4\}_2] + L^9 \xrightarrow[RT]{CHCl_3} [MoI_2(CO)_3(L^9)]$$

$$[\{WI_2(CO)_4\}_2] + L^9 \xrightarrow[RT]{CHCl_3} [WI_2(CO)_3(L^9)]$$

$$[MnCl(CO)_5] + L^9 \xrightarrow[Reflux]{CHCl_3} [\{MnCl(CO)_3\}_2(L^9)]$$

$$[ReCl(CO)_5] + L^9 \xrightarrow[Reflux]{CHCl_3} [\{ReCl(CO)_3\}_2(L^9)]$$

$$[MnBr(CO)_5] + L^9 + AgCF_3SO_3 \xrightarrow[Reflux]{Acetone} [Mn(CO)_3(L^9)](CF_3SO_3)$$

Scheme 19

There have been published *cis*- and *trans*- $[Ru^{II}X_2(L^9)]$ with X being Cl, Br, or I (*cis*-$[RuCl_2(L^9)]$[Figure 12], *trans*-$[RuCl_2(L^9)]$, *cis*-$[RuBr_2(L^9)]$, *trans*-$[RuBr_2(L^9)]$, trans-$[RuI_2(L^9)]$)[25]. NMR spectroscopy was used to confirm the compound $[RuX_2(L^9)]$'s two halogen atoms' *cis*- configuration. Despite the fact that the ionic radii of Ru^{II} and Rh^{III} are relatively comparable, the quick synthesis of the *cis*- isomer of the Ru^{II} molecule contrasts with the finding of the trans-dichloro configuration[31] of Rh^{III} in $[RhCl_2(L^9)]^+$. The Ru^{II} ion is coupled to two mutually *cis*-chlorides and four Se atoms of a bent L^9 structure in a deformed octahedral layout, according to the complex's structure. The little difference in length between Ru-Se bond *trans*- to Se and Ru-Se bond *trans*- to Cl suggests that Se has a stronger trans impact than Cl. Compared to the thioether kinds, this selenoether group has a weaker impact[32]. The *trans*- isomers of $[RuX_2(L^9)]$ (X=Cl or Br) can be made by refluxing the related *cis*-compounds in nitromethane, as opposed to $[RuX_2(L^{11})]$. Detailed characterization of the compound was not possible due to $[RuI_2(L^9)]$'s limited solubility in typical organic solvents. The NMR spectroscopy validated the *trans*- configuration. Additionally, an interaction between $[RuCl_2(PPh)_3]$ and L^9 result in the *trans*-$[RuCl(PPh_3)(L^9)](PF_6)$ [Figure 12][25]. The *trans*-orientation of Cl and PPh_3 is supported by NMR spectroscopy. The distorted octahedral architecture of this molecule is completed by mutually *trans*-Cl and PPh_3 ligands and endo-cyclically connected tetradentate Se-ether ligand. All of the methylene units are oriented to the side of the $RuSe_4$ plane that is opposite from the PPh_3 ligand because of the bulky PPh_3's steric impact, which results in an uncommon all up layout for the ligand's Se-based lone pairs. The NMR

spectra of $[OsCl(PPh_3)(L^9)](PF_6)$[25] indicated a *trans*-chloro-phosphine configuration within the octahedral Os^{II}, as found in its ruthenium counterpart. Studies using electrochemistry on metal(II) compounds revealed that the reversible M^{II}/M^{III} couple is present in all dichloro, dibromo, and chlorophosphinecompounds. *Trans*-$[RuBr_2(L^9)]$ was chemically oxidised to the appropriate Ru^{III} component by reacting the complex with Br_2-CCl_4, which produced a greenish trans- $[RuBr_2(L^9)]Br$[25].

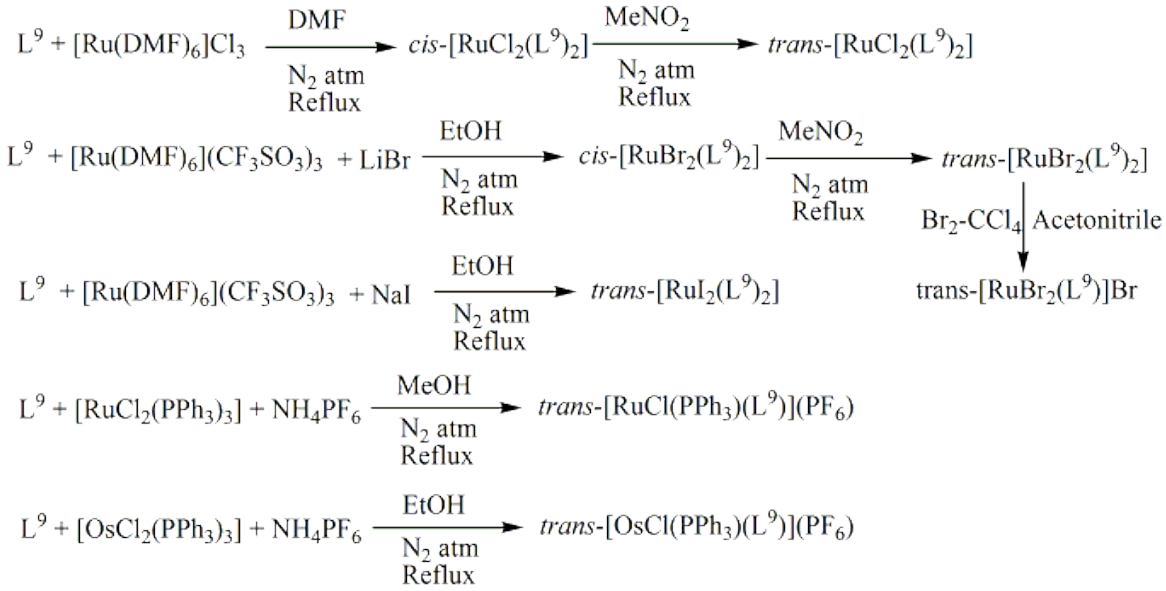

Scheme 20

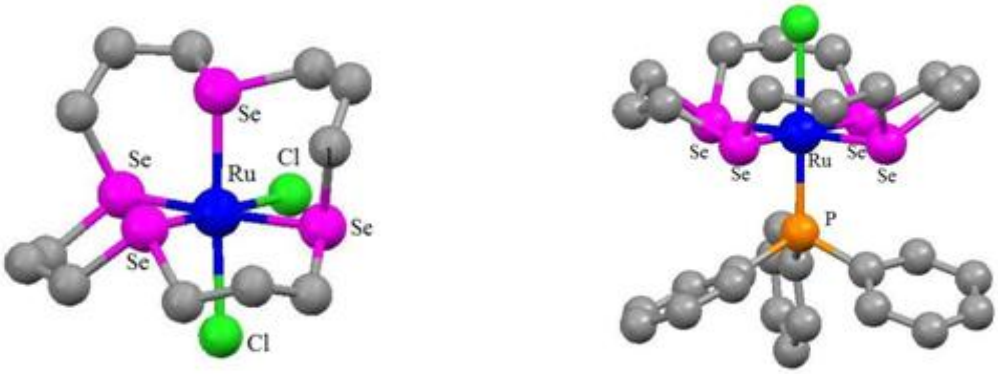

$[RuCl_2(L^9)]$ trans-$[RuCl(PPh_3)(L^9)](PF_6)$

Figure 12

The formation and characterisation of the analogous family $[MX_2(L^9)]^+$ (M= C o, X= Cl/Br/I,M= Rh/Ir, X= Cl/Br); $[CoCl_2(L^9)](PF_6)$, $[CoBr_2(L^9)](PF_6)$, $[CoBr_2(L^9)](BPh_4)$, $[CoI_2(L^9)](PF_6)$, $[RhCl_2(L^9)](BF_4)$, $[RhBr_2(L^9)](PF_6)$, $[IrCl_2(L^9)](BPh_4)$, $[IrBr_2(L^9)](BPh_4)$ have been published by researchers[26,31].Scheme 21 displays the synthetic routes of these complexes. For X = Cl or Br, $[CoX_2(L^9)]^+$ spectroscopic measurements indicate that solely the trans-forms exists, however when X =I, a combination of *cis*- and *trans*-species are available. The *cis*- and *trans*- isomers of the Rh^{III} and Ir^{III} complexes can be found in

dmf solution, according to NMR investigations. While $MeNO_2$ exclusively contains *trans*-, this is due to the two solvents' differing solubility for the *cis*- and *trans*-versions. The macrocyclic Selenium atoms inhabit the equatorial sites for coordination in the framework of the centrosymmetric $[MX_2(L^9)]^+$ (M= Co, Rh, or Ir) cations, whereas the non-bonded Se lone pairs assume up, up, down, down orientation. The macrocyclic cavity is occupied by the M^{III} ions, which have distorted octahedral shape and coordinate through two trans-halides and all available selenium donor atoms. The related thioether crown compound also displays a trans-dichloro framework, with the thioether crown filling the equatorial plane. The stereochemistry is comparable with that compound. The inability of similar attempts to produce the Co^{III} species of L^{11}, $[CoX_2(L^{11})]^+$, is due to the macrocycle L^9's higher degree of stability.

$$L^9 + CoCl_2 + NH_4PF_6 \xrightarrow[N_2\ atm,\ Reflux]{Nitromethane} [CoCl_2(L^9)](PF_6)$$

$$L^9 + CoBr_2 + NH_4PF_6 \xrightarrow[N_2\ atm,\ Reflux]{Nitromethane} [CoBr_2(L^9)](PF_6)$$

$$L^9 + CoBr_2 + NaBPh_4 \xrightarrow[N_2\ atm,\ Reflux]{Nitromethane} [CoBr_2(L^9)](BPh_4)$$

$$L^9 + CoI_2 + NH_4PF_6 \xrightarrow[N_2\ atm,\ Reflux]{Nitromethane} [CoI_2(L^9)](PF_6)$$

$$L^9 + RhCl_3.3H_2O + NaBF_4 \xrightarrow[N_2\ atm,\ Reflux]{EtOH} [RuCl_2(L^9)](BF_4)$$

$$L^9 + [Rh(H_2O)_6](NO_3)_3 + LiBr{+}NH_4PF_6 \xrightarrow[N_2\ atm,\ Reflux]{EtOH} [RuBr_2(L^9)](PF_6)$$

$$L^9 + IrCl_3.3H_2O + NaBPh_4 \xrightarrow[N_2\ atm,\ Reflux]{EtOH/H_2O} [IrCl_2(L^9)](BPh_4)$$

$$L^9 + IrBr_3.3H_2O + NaBPh_4 \xrightarrow[N_2\ atm,\ Reflux]{EtOH/dmf} [IrBr_2(L^9)](BPh_4)$$

Scheme 21

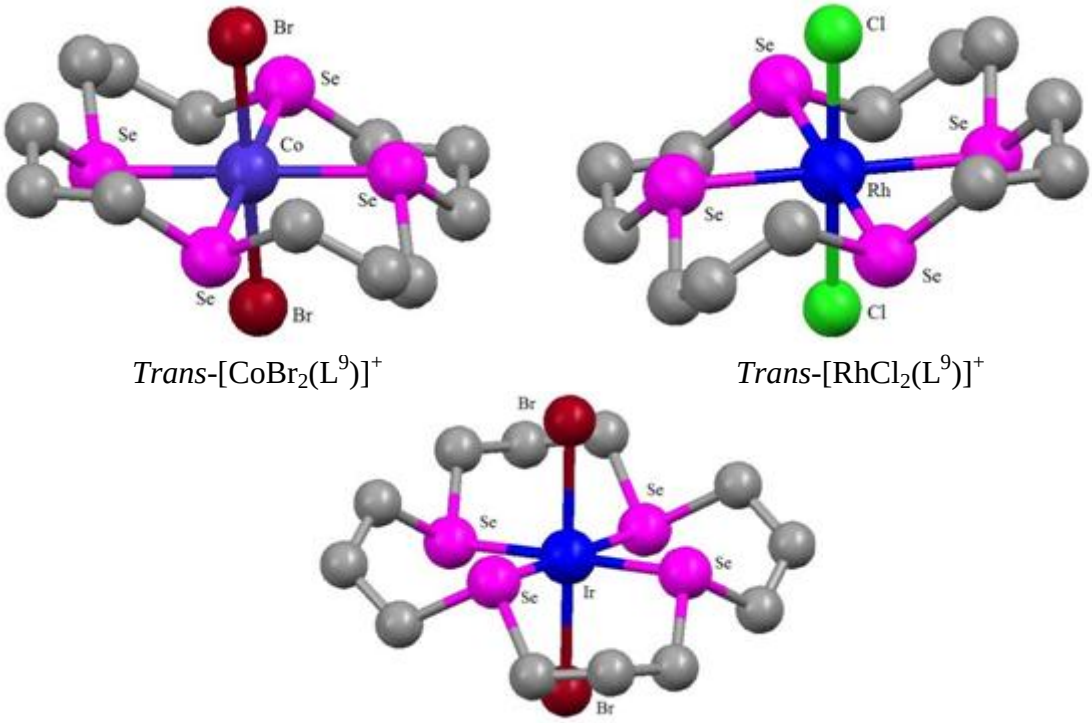

Trans-$[CoBr_2(L^9)]^+$ *Trans*-$[RhCl_2(L^9)]^+$

Trans-$[IrBr_2(L^9)]^+$

Figure 13

Because $[NiX_2(L^9)]$ is poorly soluble across the majority solvents, it was impossible to grow crystals appropriate for an X-Ray analysis. The assigning of *trans*-octahedral architectures for the paramagnetic compounds $[NiX_2(L^9)]$, [by reaction of NiX_2 (X = Cl, Br or I) with L^9], derive based on their paramagnetism and UV-Vis spectra[33].$[M(L^9)](PF_6)_2$ [M= Pd, Pt][34] was the result of the reaction between MCl_2 (M= Pd, Pt) and L^9 and $TlPF_6$. The four Se donors are placed in a square planar pattern surrounding the main metal ion in each kind, which is endocyclic. In every situation, the macrocycle assumes an *up, up*, *down*, and *down* structure. Right in the Se_4 coordination plane is where the metal ion is located. The related thioether macrocyclic compound possesses an analogous framework, which points to a comparable cavity dimension. Every M^{2+}cation has two non-coordinating acetonitrile solvent molecules attached to it. $[M(L^9)]^{2+}$ shares a general stereochemistry with the acyclic bis(bidentate) Pt^{II} compound[28].Contrary to all the other L^9 compounds, which have retained their solid state conformation in solution, variable temperatures NMR investigations for such compounds reveal the existence of invertomers[34]. Researchers prepared the Pd^{II} compounds of $L^9$with various counterions and various ligand configurations. Both the $[Pd(L^9)][BF_4]_2$ and $[Pd(L^9)](Cl)(BF_4)$ compounds have a centrally bonded Pd that is squarely linked by the four Se atoms[35]. The reactions are shown in Scheme 22 and the crystal structures of the cations are shown in Figure 14. L^9 has the potential to synthesise compounds with four distinct diastereomeric coronand configurations.

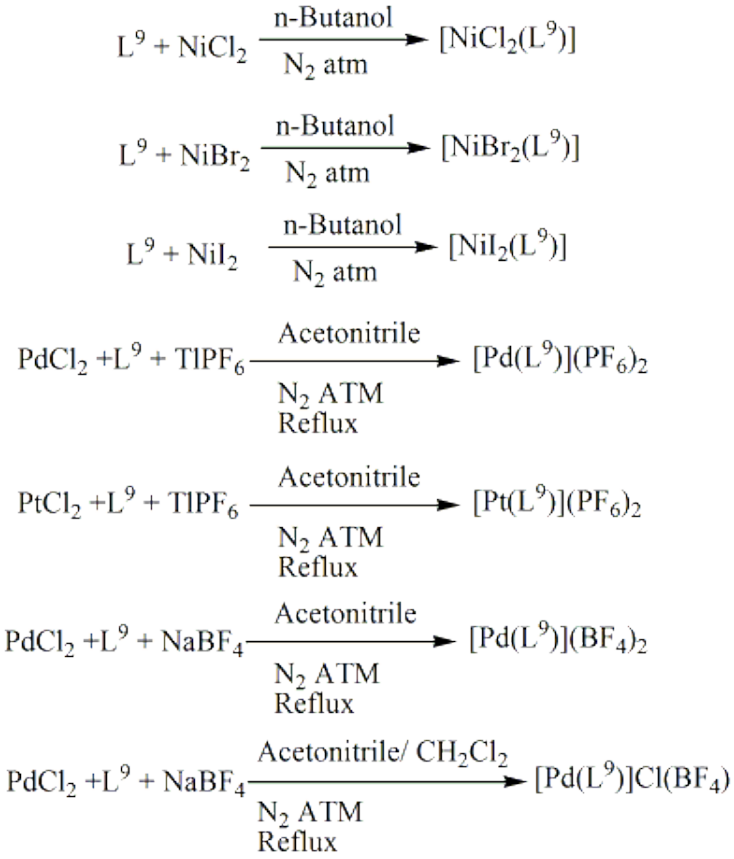

Scheme 22

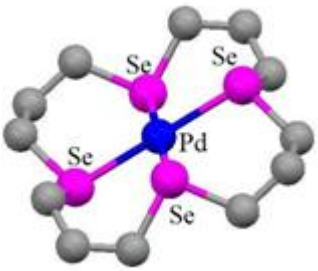

Cation of $[Pd(L^9)](PF_6)_2$

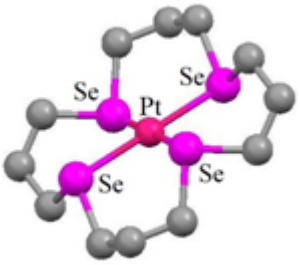

Cation of $[Pt(L^9)](PF_6)_2$

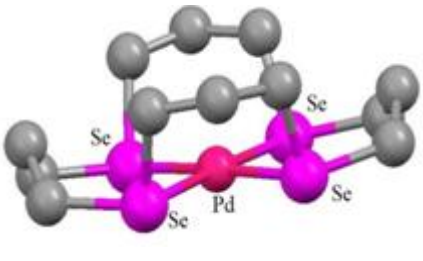

Cation of $[Pd(L^9)](BF_4)_2$

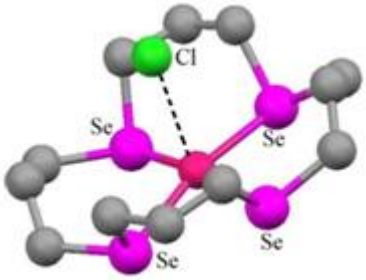

Cation of $[Pd(L^9)]Cl(BF_4)$

Figure 14

By oxidising $[Pt(L^9)][PF_6]$ with halogens, the very initial instance of the Pt^{IV} compounds $[Pt(L^9)X_2][PF_6]_2$ (X = Cl, Br) [Scheme 23] was generated[36]. The

complex's architecture proved that those octahedral entities contain the Se_4X_2 donor group and shows how the soft Se-ether macrocycle stabilise the comparatively rigid Pt^{IV} centre. In $[PtCl_2(L^9)][PF_6]_2$ [Figure 15], each of the four Se donor atoms interact equatorially with the Pt ion in a *trans*-dichloro configuration. The ligand is arranged *up, up, down*, and *down*. Investigation disproves the existence of many invertomers, as predicted by the Pt^{II} antecedent in solution[34], and instead reveals the existence of a single invertomer that is comparable to the other octrahedral compounds.

$$[Pt\text{-}(L^9)][PF_6] + Cl_2 \text{ (in CCl4)} \xrightarrow{\text{Acetonitrile}} [Pt(L^9)Cl_2][PF_6]_2$$

$$[Pt\text{-}(L^9)][PF_6] + Br_2 \text{ (in CCl4)} \xrightarrow{\text{Acetonitrile}} [Pt(L^9)Br_2][PF_6]_2$$

Scheme 23

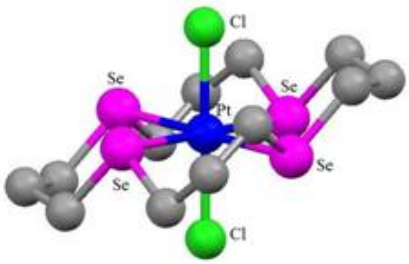

Figure 15

Alkyl-(chalcogenoether) transition metal complexes have uncommon reaction chemistry. By reacting $[PtMe_2(SMe_2)_2]$[29] with L^9, the first planar $[Me_2(Se\text{-ether})Pt^{II}]$ compound $[PtMe_2(L^9)]$ was produced. Microanalysis and positive ion electrospray Mass Spectroscopy tests provided confirmation to the composition. Being relatively unstable, this Pt^{II} combination disintegrates regardless of being kept under Nitrogen atmosphere. The earliest instance of an alkyl Pt^{IV} compound with macrocyclic selenoether coordination is the distorted octahedral complex, $[PtMe_3I(\kappa^2\text{-}L^9)]$. When $[PtMe_3I(\kappa^2\text{-}L^9)]$ was treated with $TlPF_6$, iodide was cleanly abstracted, yielding $[PtMe_3(\kappa^3\text{-}L^9)](PF_6)$[27]. This is a very uncommon instance of a Se-ether-coordinated cationic $[(alkyl)Pt^{IV}]$ compound. Due to the extremely powerful ligand field that the Me ligands within the Pt^{IV} species offer, the Pt^{IV} compound becomes more persistent than the Pt^{II} species. Due to its coordinative saturation, this molecule offers little chance for Se-C bond breakage with the aid of metals.

$$[PtCl_2(SMe_2)_2] \xrightarrow[Et_2O]{\text{MeLi}} [PtMe_2(SMe_2)_2] \xrightarrow[H_2O\ rt]{L^9} [PtMe_2(L^9)]$$

Ice-Cold Suspension

$$[PtMe_3I] + L^9 \xrightarrow{CHCl3} [PtMe_3I(\kappa^2\text{-}L^9)] \xrightarrow[CHCl_3\ N_2\ atm]{TlPF_6} [PtMe3(\kappa^3\text{-}L^9)](PF_6)$$

Scheme 24

The initial Cu^{II} compound of L^9 was, $[Cu(L^9)(SO_3CF_3)_2]$[37]. This Cu^{II} structure and the analogous thiaether compound are architecturally identical[38]. The structure has *trans*-axial triflate donors and a tetragonally deformed octahedral shape at Cu. In coordinating organic solvents, the compound experiences an unusual the transfer of electrons that yields $[Cu(L^9)][SO_3CF_3]$ (polymeric Cu^I compound), intermediate radical cation $[L^9]^{+\bullet}$, and the stable dication $[L^9]^{2+}$. The L^9dication's architecture differs greatly from L^9's in several ways. Three Se atoms are almost aligned within the $[L^9]^{2+}$ dication, which allows the "+" charges on the two exterior Se atoms to best separate. The "+" charges are distributed amongst the four Se atoms thanks to a weak secondary interaction between the 4th and centre Se atoms. Pseudo-trigonal-bipyramidal arrangement of the bonds is around the core Se atom. The longer Se.....O and Se.....F lengths imply that the cation and anion are electrostatically attracted to one another in a dipolar fashion. The selenium coronand dication produced by an electron-transfer interaction within a metal-selenium coronand compound was first documented in this study. According to data from UV-Vis spectroscopy, cyclic voltammetry, spectroelectrochemistry, and coulometry, of the reaction's intermediates[39], $[L^9]^{+\bullet}$ and $[L^9]^{2+}$, it was concluded that L^9 is first oxidised to $[L^9]^{+\bullet}$ and subsequently to $[L^9]^{2+}$. The conjugate $[Cu(L^9)](SO_3CF_3)$[40] is produced via the interaction of $[Cu^I(SO_3CF_3)]$ with L^9. In contrast to the cyclic polythia ether compounds of Cu^I and Cu^{II}, the Cu^I compound of L^9here is not enclosed by L^9. Each Cu^+ ion in the compound is pseudo-tetrahedrally linked by four separate Se atoms from L^9 rings. The complex cation and the anion $SO_3CF_3^-$ hardly ever make any notable interactions. The unusual lattice stability connected to the selection of anion and the low energy configuration of L^9 ring were said to be the causes of the production of the particular type of Cu^I complex. Cu-Se bond distances are slightly greater than the Cu-S bond lengths for Cu^I compounds of cyclic polythia ethers. The Ag^I compound was produced[21] via the interaction of $AgBF_4$ with L^9. The compound is assumed to have a polymeric structure comparable to the Cu^I counterpart in the solid state due to its lack of solubility in organic solvents.

$$L^9 + [Cu^{II}(CF_3SO_3)] \xrightarrow[10\ min]{Acetone} [Cu(L^9)(CF_3SO_3)_2]$$

$$2\,[Cu(L^9)(CF_3SO_3)_2] + L^9 \xrightarrow[N_2\ atm,\ 5\ min]{CH_2Cl_2/CH_3CN} 2\,[Cu(L^9)](CF_3SO_3) + [L9]^{2+}(CF_3SO_3)_2$$

$$L^9 + [Cu^{I}(CF_3SO_3)] \xrightarrow[N_2\ atm,\ 3\ hr]{CH_2Cl_2/CH_3CN} [Cu(L^9)](CF_3SO_3)$$

Scheme 25

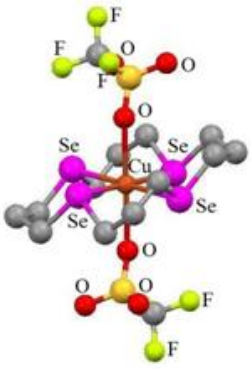

$[Cu(L^9)(SO_3CF_3)_2]$

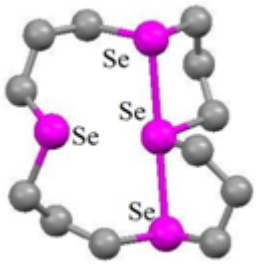

$[L^9]^{2+}$

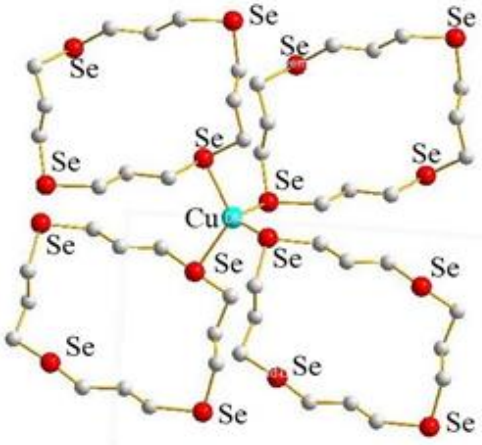

Sectional view of polymeticcation of $[Cu(L^9)][SO_3CF_3]$

Figure 16

L^9 and $Hg(CN)_2$ interact to form a compound, where tetragonally deformed octahedral ligand framework surrounds the Hg atom. The arrangement of the molecules allows four Se atoms from the four separate rings to coordinate Hg in a plane that is roughly perpendicular to the $Hg(CN)_2$ molecular axis. The structure is shown in Figure 17[40].

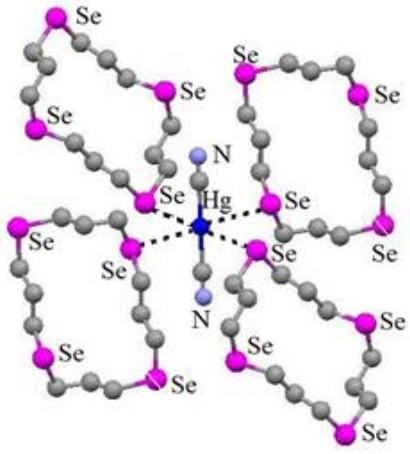

Figure 17

$([PdCl)_2(L^{10})])[BF_4]_2$ is the first reported binuclear compound, where L^{10} tridentately bonds with two separate Pd^{II} ions while chloride occupying the fourth linkage site to create $[(PdCl)_2(L^{10})]^{2+}$. The surroundings of both Pd were roughly square planar. No intra-molecular processes exist, in between Pd^{II} ions, or between one Pd^{II} ion and Cl^- bonded to other Pd^{II} ion. This structure exhibits, because of the binuclear structure of L^{10} and the potential for direct or ligand-mediated metal-metal interactions, the chemistry is particularly fascinating[35].

$$L^{10} + PdCl_2 + NaBF_4 \xrightarrow[N_2\ atm]{MeCN} ([PdCl)_2(L^{10})])[BF_4]_2$$

Scheme 26

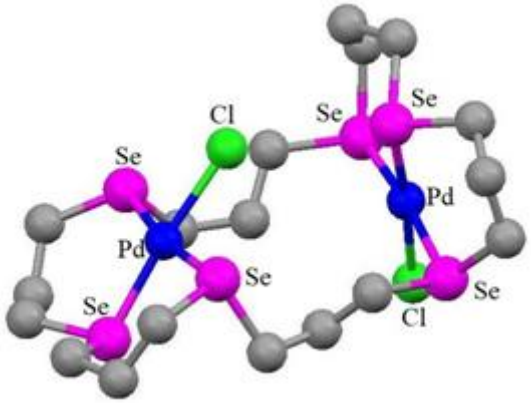

$[(PdCl)_2(L^{10})]^{2+}$

Figure 18

L^{28} reacts with M^{II} species (M=Mo or W), resulting in the formation of seven-coordinated $[MX_2(CO)_3L]$ (M=Mo, X=Br or I; M=W, X=I) products[23]. These substances degrade quickly in coordinating solvents but are poorly soluble in hydrocarbons and chlorocarbons. MCl_2 (M= Pd or Pt) interacts with L^{28} produced the neutral compound $[MCl_2(L^{28})]$[21]. The mononuclear $[PdCl_2(L^{28})]$ architecture possesses the anticipated *cis*-Cl setup, and the distorted square planar shape is completed by L^{28}. In contrary to the boat configuration in the Cu^I and Ag^I compounds, the six-membered chelate ring is in a chair configuration in this species. The composition of $[Cu(L^{28})_2](BF_4)$[21], isolated Cu^I monomer, contain two binding L^{28} ligands that provide distorted-tetrahedral configuration. The $[Cu(L^{28})_2]^+$ cation's two six-membered chelate rings are arranged in a boat shape. The configuration is comparable to related AgI compound $[Ag(L^{28})_2](BF_4)$. The increasing M-Se distances (M= Pd, Cu, and Ag) and increasing M^I radius are related. Additionally reported is $[(AuCl)_2(L^{28})]$[21]. The crustal structures are shown in Figure 19.

$$[\{MoBr_2(CO)_4\}_2] + L^{28} \xrightarrow[\text{Room temp}]{CH_2Cl_2} [MoBr_2(CO)_3(L^{28})]$$

$$[\{MoI_2(CO)_4\}_2] + L^{28} \xrightarrow[\text{Room temp}]{CH_2Cl_2} [MoI_2(CO)_3(L^{28})]$$

$$[\{WI_2(CO)_4\}_2] + L^{28} \xrightarrow[\text{Room temp}]{CH_2Cl_2} [WI_2(CO)_3(L^{28})]$$

$$[Cu(MeCN)_4](BF_4) + L^{28} \xrightarrow[N_2\ atm,\ RT]{Acetatone} [Cu(L^{28})2](BF_4)$$

$$AgBF_4 + L^{28} \xrightarrow[N_2\ atm,\ RT]{Acetatone} [Ag(L^{28})2](BF_4)$$

$$[AuCl(tht)] + L^{28} \xrightarrow[N_2\ atm,\ RT]{Acetatone} [AuCl_2(L^{28})]$$

(tht = tetrahydothiophene)

$$PdCl_2 + L^{28} \xrightarrow{\text{Degassed MeCN}} \text{cis-}[PdCl_2(L^{28})]$$

$$PtCl_2 + L^{28} \xrightarrow{\text{Degassed MeCN}} \text{cis-}[PtCl_2(L^{28})]$$

Scheme 27

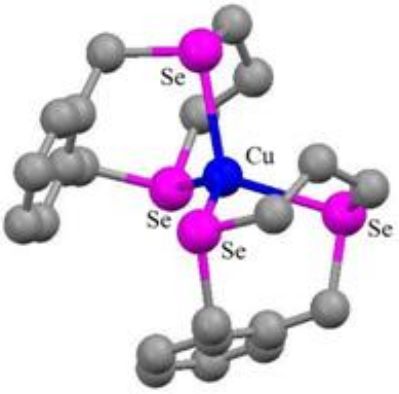

Cation of $[Cu(L^{28})_2](BF_4)$

Cation of $[Ag(L^{28})_2](BF_4)$

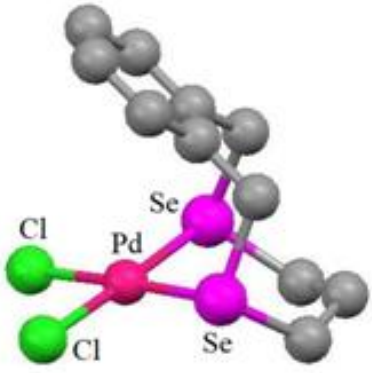

Cation of $[PdCl_2(L^{28})]$

Figure 19

The -OH groups of the coronand ligand form a reciprocal cis- connection, as evidenced by the crystal framework of the compound[13] $[Cu(L^{16})][SO_3CF_3]_2$. Just a single -OH group can bind to the Cu^{II} core due to this stereochemical arrangement, forcing the corresponding Se-Cu-Se-C-C ring into a boat shape. Cu^{II}'s linkage surroundings can also be thought of as roughly tetragonally deformed octahedral, with an "O" atom belonging to the -OH group and an "O" atom from SO_3CF_3 holding each of the pseudoaxial sites. H-bond is formed between the non-coordinated -OH group and an "O" atom of the $SO_3CF_3^-$ ion. The Cu^{II} compound of L^{17} can be recrystallized to produce a combination of the brown crystals of the Cu^{II} compound and the white crystals of the Cu^{I} compound $[Cu(L^{17})][SO_3CF_3]$[13]. The tetrahedral Se_4 donor group at Cu^{I} is distorted in the structure, and there is no -OH coordination. Similar efforts to combine L^{18} and $Cu(SO_3CF_3)_2$ to create a Cu^{II} compound of L^{18} were unsuccessful. The structure of the $[Cu(L^{15})_2][SO_3CF_3]_2$ compound[13] is roughly tetragonally distorted, with the -OH group's "O" atoms holding the weaker axial sites. H-bonds are created between the $–OH^-$ groups and the $SO_3CF_3^-$ anions nearby.

$$Cu(SO_3CF_3)_2 + L^{15} \xrightarrow{CH_3NO_2} [Cu(L^{15})_2][SO_3CF_3]_2$$

$$Cu(SO_3CF_3)_2 + L^{16} \xrightarrow{\text{Acetone}} [Cu(L^{16})][SO_3CF_3]_2$$

$$Cu(SO_3CF_3)_2 + L^{17} \xrightarrow{CH_2Cl_2} [Cu(L^{17})][SO_3CF_3]_2$$

Scheme 28

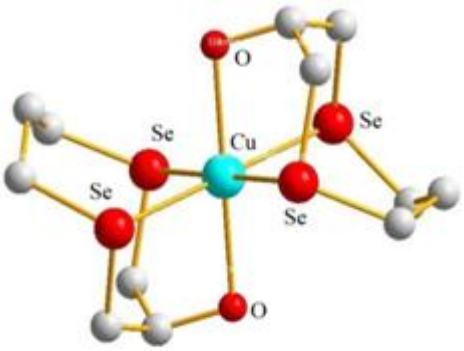

Cation of $[Cu(L^{15})_2][SO_3CF_3]_2$

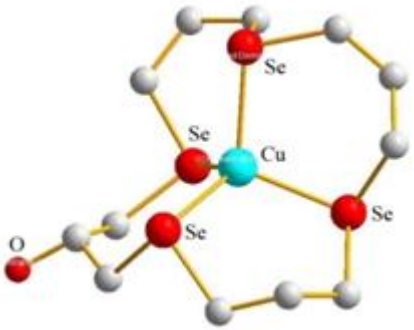

Cation of $[Cu(L^{17})][SO_3CF_3]$

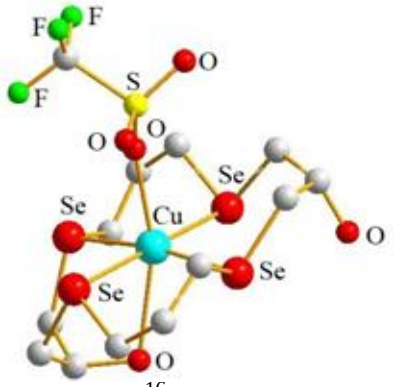

$[Cu(L^{16})][SO_3CF_3]_2$

Figure 20

L^{26} produced $[Re_2(CO)_9(L^{26})]$ and polymer $[Cu_4I_4(\mu-\eta^2-L^{26})_2]$ as products of reactions with $[Re_2(CO)_9(NCMe)]$ and CuI, respectively[19]. $[Cu_4I_4(\mu-\eta^2-L_{26})_2]$ exhibits a three-dimensional network of Cu_4I_4 units that resemble cubanes, connected via four bridging Se_3 crowns. Every Cu^I ion binds to one η^1 Se-ether. The L^{26} units employ an additional Se atom to connect to a nearby Cu^I, keeping the third Se atom uncoordinated. The figures are shown in Figure 21.

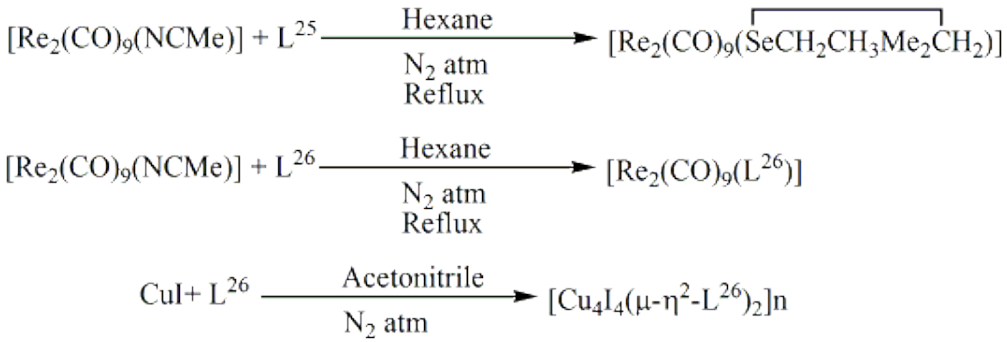

Scheme 29

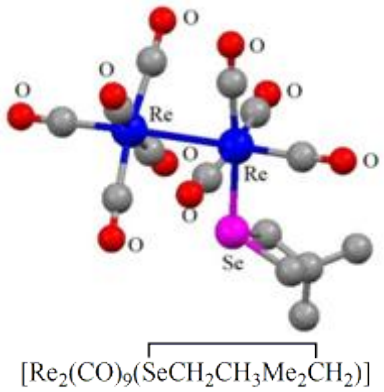

$[Re_2(CO)_9(SeCH_2CH_3Me_2CH_2)]$

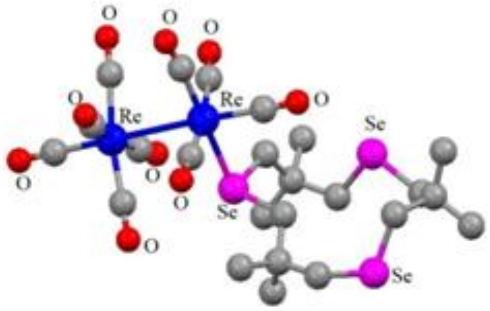

$[Re_2(CO)_9(L^{26})]$

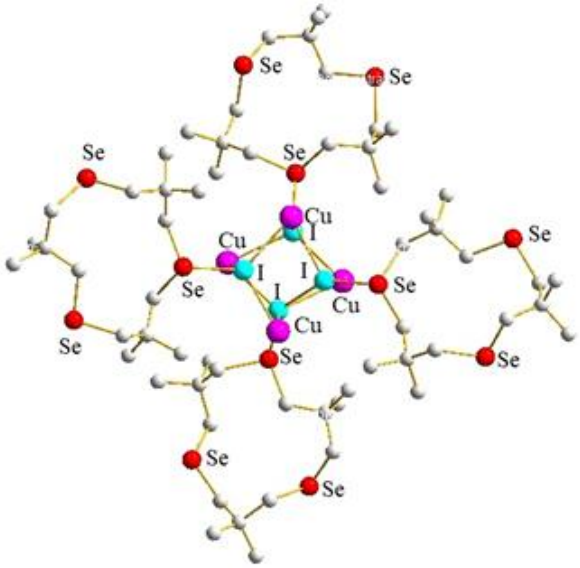

Subunit of $[Cu_4I_4(\mu-\eta^2-L^{26})_2]$

Figure 21

- **With p-block Elements:** Coordination chemistry of main group elements has regularly obtained less focus than transition metals, probably because the compounds tend to lack several of the properties needed to facilitate characterization by standard spectroscopic techniques. Researchers investigated the chemistry of coordination between group 15 metal ions [As, Sb, Bi] and macrocyclic Se-ether ligands. These ions easily combine with macrocyclic Se-ether ligands to produce a wide variety of unique, occasionally polymeric structural patterns. These motifs are based on several collective factors like primary M-X (X = Cl/ Br/ I) associations and a sequence of secondary M.....Se, and occasionally M.....X interactions.

$[(AsCl_3)_4(L^{10})]$[41] is the very first illustration of a macrocyclic Se-ether compound of a nonmetallic component. Four $AsCl_3$ components per Se_6-ether macrocycle is an extremely rare combination visible in the framework. Two $AsCl_3$ components connect *exo*- to the ring through just one Se atom and the remaining two create a loosely attached dinuclear μ^2-chloro bridged component *endo*- to the ring, with every As atom bonded to two *cis*-Se atoms from L^{10}. Thus, the macrocycle's entire six Se atoms link to the As centres. It is extremely unusual and novel to see *exo*- and *endo*-coordination in a single macrocyclic complex as well as the presence of a dinuclear M_2X_6 segment inside the ring. As ions located inside and outside the ring have different configuration around it, as well as coordination numbers. At every As centre within the ring, two *cis*- Se atoms from the ring and four Cl^- create a distorted octahedral geometry. Considering there is no notable deviation from the values anticipated for an octahedron, the stereochemical behaviour of the lone pair located at As centres (*endo*- to the ring) is not apparent right away. The interaction of three terminal Cl^-, one Se atom within the ring, and the stereochemically active lone pair of electrons results in the distorted sawhorse configuration of As (*exo*- to the ring). Additionally published is a 2:1 compound, $[(AsBr_3)_2(L^{10})]$[42]. $[BiX_3(L^{10})]$[43] is produced when BiX_3 [X = Br or Cl] reacts with L^{10}. Nevertheless, incomplete characterisation was not achieved due to its weak solubility. The figure of $[(AsCl_3)_4(L^{10})]$ shown in Figure 22.

$$AsCl_3 + L^{10} \xrightarrow{\text{anh. } CH_2Cl_2} [(AsCl_3)_4(L^{10})]$$

$$AsBr_3 + L^{10} \xrightarrow{\text{anh. } CH_2Cl_2} [(AsBr_3)_2(L^{10})]$$

$$BiCl_3 + L^{10} \xrightarrow{CH_3CN} [BiCl_3(L^{10})]$$

$$BiBr_3 + L^{10} \xrightarrow{CH_3CN} [BiBr_3(L^{10})]$$

Scheme 30

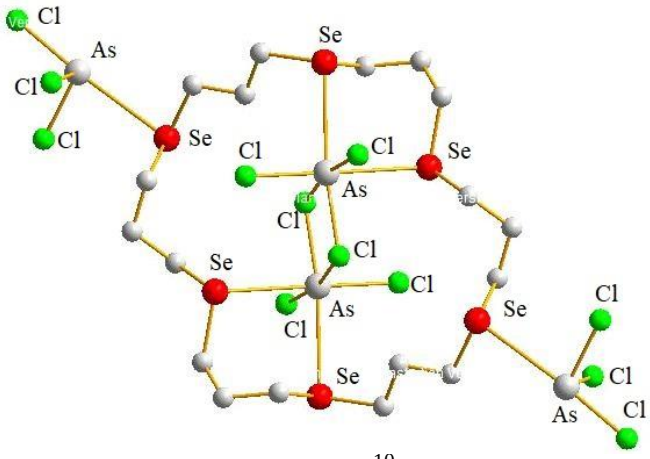

$[(AsCl_3)_4(L^{10})]$

Figure 22

Solid compounds having a 2:1 M to L^9 stoichiometry was produced by the interaction of MX_3 with L^9 (where X is Cl/Br/I, and M is As/Sb/Bi). Due to the molecules' weak solubility in non-coordinating solvents and the Se-ether ligand's fast replacement in the coordinating solvent, their characterization was hindered. Equivalent 3D sheet polymer frameworks containing five-coordinate As^{III} linked to three terminal chlorides or bromides and two *cis*-Se donor atoms from *exo*-coordination towards two distinct macrocyclic rings may be seen in the As^{III} Br and Cl complexes. This five-coordinate structure resembles octahedral shape that has an empty vertex that was thought to be filled by the As-based lone pair[42]. The figures are shown in Figure 23.

$$AsCl_3 + L^9 \xrightarrow{CH_2Cl_2} [(AsCl_3)_2(L^9)]$$
$$AsBr_3 + L^9 \xrightarrow{CH_2Cl_2} [(AsBr_3)_2(L^9)]$$

Scheme 31

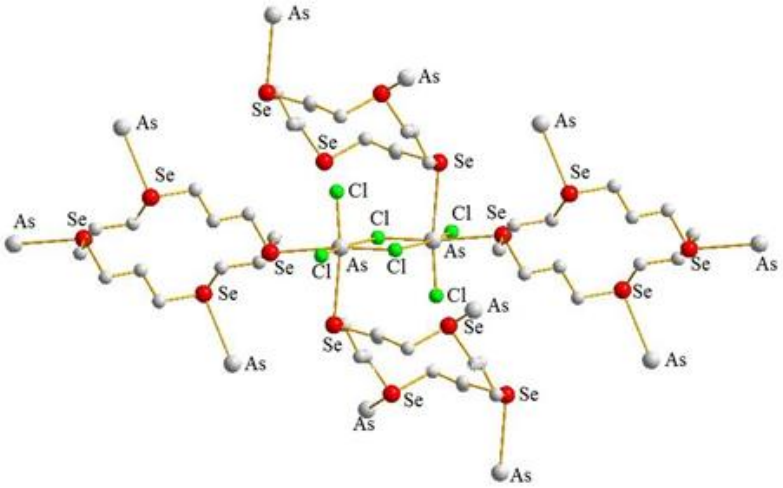

$[(AsCl_3)_2(L^9)]$

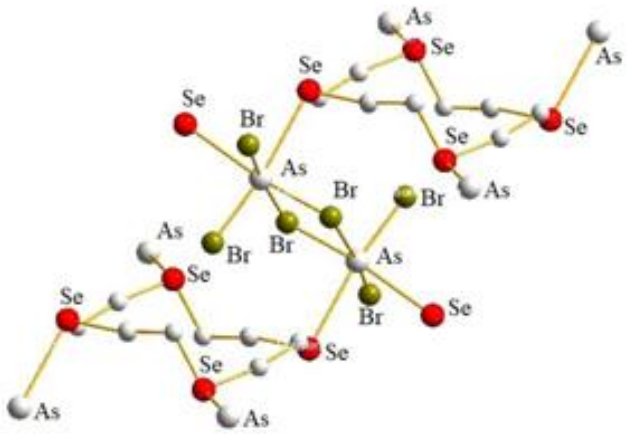

$[(AsBr_3)_2(L^9)]$

Figure 23

In $[(SbBr_3)_2(L^9)]$[44], L^9 ligands connected *exo*-cyclically to four Sb centres, each of which bridges to a different Se-crown. In order to establish a distorted square pyramidal coordination surroundings, the structure at Sb can be represented having five coordination via primary contacts to three *fac*- terminal bromide and additional interactions to two *cis*- Se atoms from separate macrocycles. The persistence of the pyramidal $SbBr_3$ unit seen in the parent antimony trihalide plus the existence of weak secondary Sb-Se connections on the opposite face, which results in the Se atoms sharing adjacent *cis*- coordination locations, constitute the key characteristics of this molecule. $[(SbCl_3)_2(L^9)]$ and $[(SbI_3)_2(L^9)]$ are also reported[45].

$$SbCl_3 + L^9 \xrightarrow{CH_3CN} [(SbCl_3)_2(L^9)]$$

$$SbBr_3 + L^9 \xrightarrow{CH_3CN} [(SbBr_3)_2(L^9)]$$

$$SbI_3 + L^9 \xrightarrow{CH_3CN} [(SbI_3)_2(L^9)]$$

Scheme 32

$[(SbBr_3)_2(L^9)]$

Figure 24

Based on nearly planar Bi_2Br_6 parts, $[BiBr_3(L^9)]$ assumes a one-dimensional ladder configuration, with each Bi of the following Bi_2Br_6 groups is connected by bridging L^9 ligands[43]. One Se donor atom is used to coordinate with each Bi, creating a μ-bridging L^9. The macrocycles take on an exocyclic shape and are joined by mutually *trans*-selenium donors. Donor's set *trans*-Se_2Br_4 coordinates each Bi. In each L^9 unit, remaining two Se atoms that are mutually *trans*- continue to be uncoordinated. Such molecular configurations stand contrary to those discovered for the Sb^{III} and As^{III} counterparts, which exhibit linkage *via* two mutually *cis*- Se atoms that come from different macrocycles and are architecturally quite similar. L^9 and SnX_4 interact to produce the 1:1 compounds $[SnX_4(L^9)]$ (X = Cl/Br)[46]. The spectroscopic findings are in favour of a 1:1 combination containing a bent Cl_4Se_2 octahedral donor positioned at Sn centre.

$$BiCl_3 + L^9 \xrightarrow{MeCN/CH_2Cl_2} [BiCl_3(L^9)]$$

$$BiBr_3 + L^9 \xrightarrow{MeCN/CH_2Cl_2} [BiBr_3(L^9)]$$

$$SnCl_4 + L^9 \xrightarrow[CH_2Cl_2]{\text{Degassed}} [SnCl_3(L^9)]$$

$$SnBr_4 + L^9 \xrightarrow[CH_2Cl_2]{\text{Degassed}} [SnBr_3(L^9)]$$

Scheme 33

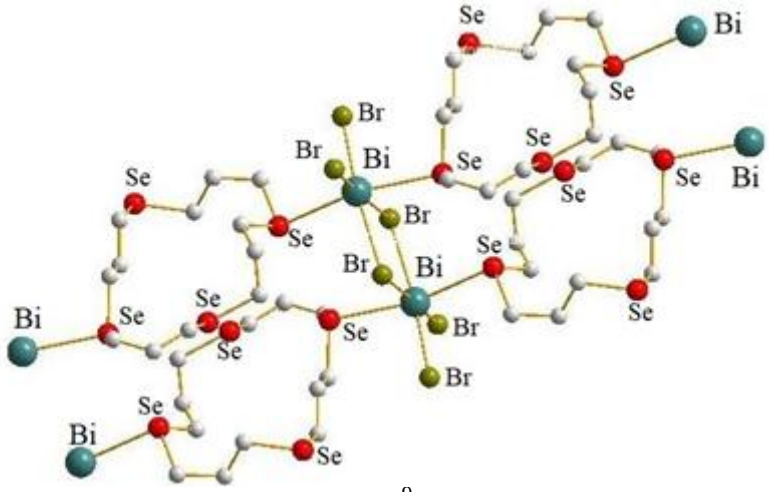

$[BiBr_3(L^9)]$

Figure 25

When MX_3 [X = Cl/Br/I and M = As/Sb/Bi] interacted with L^{11}, compounds with the empirical formula $[MX_3(L^{11})]$ were produced. It was challenging to collect significant spectoscopic information because of the compounds' weak solubility, which is probably related to their polymeric composition. $[AsCl_3(L^{11})]$ assumes a near-planar As_2Cl_6 group architecture that is connected by bridging L^{11} ligands that possess mutual *trans*- coordination spots[42,47]. The angles formed at As^{III} are quite similar to what is anticipated by a typical octahedron.

$$AsCl_3 + L^{11} \xrightarrow{CH_2Cl_2} [AsCl_3(L^{11})]$$
$$AsBr_3 + L^{11} \xrightarrow{CH_2Cl_2} [AsBr_3(L^{11})]$$
$$AsI_3 + L^{11} \xrightarrow{CH_2Cl_2} [AsI_3(L^{11})]$$

Scheme 34

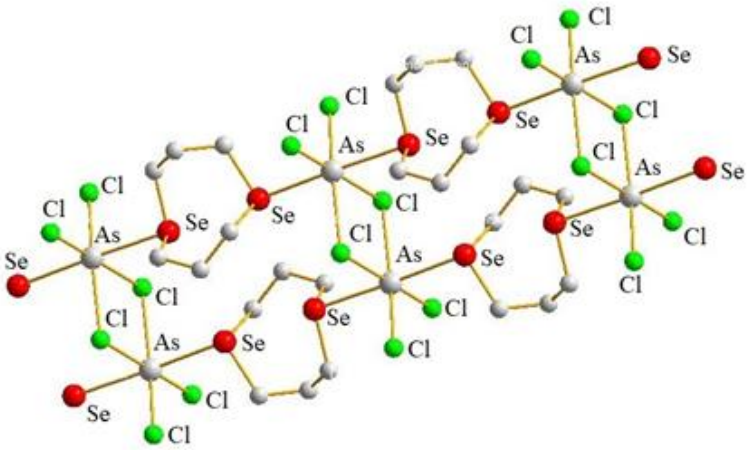

$[AsCl_3(L^{11})]$

Figure 26

$[BiCl_3(L^{11})]$[43] architecture exhibits an endless one-dimensional ladder arrangement made of almost planar Bi_2Cl_6 connected by four bridging L^{11}. On every Bi ion, the Se-donor atoms utilise mutually *trans*- coordination positions. The $[SbCl_3(L^{11})]$[47] complex crystallises as edge-bridged square pyramids containing *anti*-L^{11} ligands, or $[Sb_2Cl_6(\eta^1\text{-}L^{11}]$ dimers. The rest of the Se atoms participate in further long-range Sb-Se contacts that connect the dimers into endless ladder architecture. It is strikingly comparable to that found in the As^{III} and Bi^{III} analogues.

$$BiCl_3 + L^{11} \xrightarrow{CH_3CN/CH_2Cl_2} [BiCl_3(L^{11})]$$

$$BiBr_3 + L^{11} \xrightarrow{CH_3CN/CH_2Cl_2} [BiBr_3(L^{11})]$$

Scheme 35

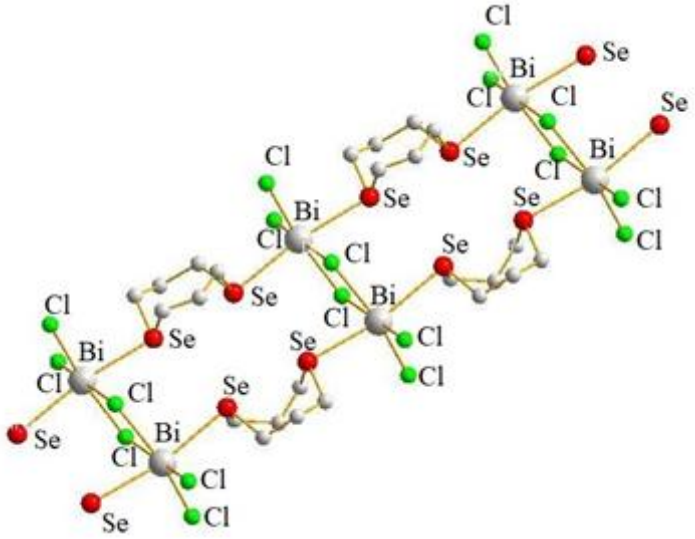

$[BiCl_3(L^{11})]$

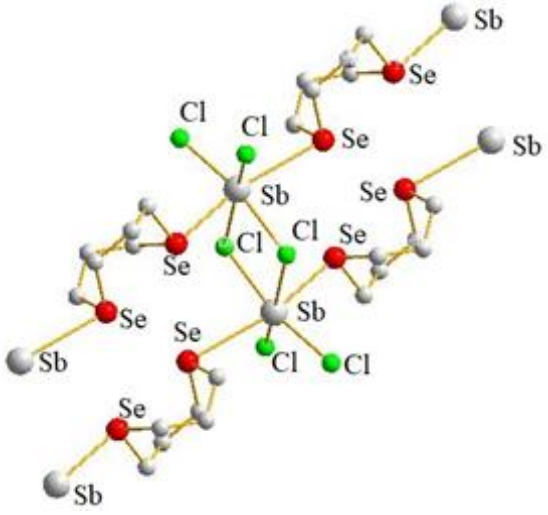

$[SbCl_3(L^{11})]$

Figure 27

Straightforward comparison of the building blocks is possible thanks to the accessibility of the crystal structure information of all of these related Se-ether compounds. As compared to the As and Bi compounds, which both have significantly more conventional six-coordinate designs, the Sb compound has severely distorted (5+1)-coordination. The different degrees of stereochemical orientation of the metal-based lone pair in those complexes may be the cause of the structural variations. The As^{III} complex's uniform shape and the lengthening each of the As-Cl and As-Se bond lengths by about identical amounts point to the lone pair's stereochemical inactivity. For pseudo 7-coordination (either 7 ligands or 6 ligands and one lone pair), As is too small in size. Indicating stereochemical inactivity as well as the likelihood for a Bi-based lone pair inhabiting the 6s orbital is consistent 6-coordination at Bi centre with no appreciable alteration of the bond distances and angles. The distorted bond distances and angles surrounding Sb indicate that the lone pair based on Sb is stereochemically directed and localised in the plane.

IV. CONCLUSION

The complex yet intriguing coordination chemistry of macrocyclic poly-Se ethers led to the emergence of its science. Synthesis of selenium-macrocycles in addition to studies of their coordination chemistry has attracted quite a bit of attention. Scientists have created new homo as well as mixed donor Se-ether macrocyclic compounds and are primarily interested in how these substances attach to transition/non-transition metal ions. The synthetic process of coronand macrocycles, which contain only Se donor atoms, as well as their metal complex preparation methodologies and multiple crystal frameworks are all addressed in this chapter. Selenocyclophanes were additionally briefly discussed also.

REFERENCES

[1] C.J. Pedersen, “Cyclic polyethers and their complexes with metal salts”, J. Am. Chem. Soc., Vol. 89, pp. 7017–7036, 1967.

[2] (a) J.M. Lehn, “Design of organic complexing agents Strategies towards properties”, Struct. Bond. (Berl.) Vol. 16, pp. 1-69, 1973. (b) J.M. Lehn, “Supramolecular Chemistry—Scope and Perspectives Molecules, Supermolecules, and Molecular Devices (Nobel Lecture)”, Angew. Chem. Int. Ed. Engl., Vol. 27, pp. 89-112, 1988.

[3] D.J. Cram, “The Design of Molecular Hosts, Guests, and Their Complexes (Nobel Lecture)”, Angew. Chem. Int. Ed. Engl., Vol. 27,pp. 1009-1020, 1988.

[4] R.H. Mitchell, “The synthesis and reactions of 2,11-diselena[3,3]metacyclophanes. An investigation of the selenoxide elimination route to metacyclophane-1,8-dienes”, Can. J. Chem., Vol. 58, pp. 1398-1406, 1980.

[5] H. Higuchi and S. Misumi, “Deselenation of diselenacyclophanes —a new synthetic method of [2.2]cyclophanes”, Tetrahedron Lett., Vol. 23, pp. 5571-5574, 1982.

[6] L. R. Hanton and T. Kemmitt, “Derivatizedcyclophane chemistry. Synthesis of new (.pi.-benzene)ruthenium(II) complexes of 2,11-dithia- and 2,11-diselena[3.3]orthocyclophane”, Inorg. Chem., Vol. 32, pp. 3648-3653, 1993.

[7] S. Muralidharan, M. Hojjatie, M. Firestone and H. Freiser, “Structural and complexation properties of 2,11-diselena[3.3](2,6)pyridinophane”, J. Org. Chem., Vol. 54, pp. 393-399, 1989.

[8] M. Hojjatie, S. Muralidharan and H. Freiser, “Synthesis and multinuclear NMR characterizations of some [3.3]diselena- and [4.4]tetraselenacyclophanes”, Tetrahedron, Vol. 45, pp. 1611-1622, 1989.

[9] B. M. Pinto, B. D. Johnston, R. J. Batchelor, F. W. B. Einstein and I. D. Gay, “Selenium coronands. A novel conformational pair”, Can. J. Chem., Vol. 66, pp. 2956-2958, 1988.

[10] B. M. Pinto, B. D. Johnston, R. J. Batchelor and J. -H. Gu, “Solution conformation and pseudorotational barriers of 1,3,7,9-tetraselenacyclododecane and its 5,5,11,11-tetramethyl derivative”, J. Chem. Soc. Chem. Commun., Issue 16, pp. 1087-1089, 1988.

[11] R. J. Batchelor, F. W. B. Einstein, I. D. Gay, J. -H. Gu, B. D. Johnston and B. M. Pinto, "Selenium coronands: synthesis and conformational analysis", J. Am. Chem. Soc., Vol. 111, pp. 6582-6591, 1989.

[12] I. Cordova-Reyes, E. Vanden Hoven, A. Mohammed and B. M. Pinto, "Stepwise synthesis of selenium coronands containing an odd number of selenium atoms: 1,5,9-triselenacyclododecane and 1,5,9,13,17-pentaselenacycloeicosane", Can. J. Chem. Vol. 73, pp. 113-116, 1995.

[13] R. J. Batchelor, F. W. B. Einstein, I. D. Gay, J. -H. Gu, S. Mehta, B. M. Pinto and X. -M. Zhou, "Synthesis, Characterization, and Redox Behavior of New Selenium Coronands and of Copper(I) and Copper(II) Complexes of Selenium Coronands", Inorg. Chem., Vol. 39, pp. 2558-2571, 2000.

[14] I. Cordova-Reyes, H. Hu, J.-H. Gu, E. VandenHoven, A. Mohammed, S. Holdcroft and B.M. Pinto, "Synthesis and characterization of polymer-bound selenium coronands: enhancing the stability of reactive dications by restricting intermolecular interactions", Can. J. Chem., Vol. 74, pp. 533-543, 1996.

[15] H. Fujihara, M. Yabe, J. -J. Chiu and N. Furukawa, "Peri interaction between selenium atoms in dinaphtho[1,8-b,c]-1,5-diselenocin and 1,8-bis(methylseleno)naphthalene" Tetrahedron Lett., Vol. 32, pp. 4345-4348, 1991.

[16] H. Fujihara, M. Yabe, M. Ikemori and N. Furukawa, "Preparation and X-ray structure of 8,9,19,20-tetra hydrodinaphtho[1′,8″jk; 1,8-bc][1,5,9,13]tetraselenacyclohexadecine, and its novel ring contraction in concentrated sulfuric acid", J. Chem. Soc. Perkin Trans. 1, Issue 18, pp. 2145-2146, 1993.

[17] H. Fujihara, M. Yabe and N. Furukawa, "Synthesis, electrochemical and chemical oxidations, and peri selenium participation of macrocyclicpolyselenides containing naphthalene rings", J. Chem. Soc. Perkin Trans. 1, Issue 15, pp. 1783-1785, 1996.

[18] R.D. Adams and K.T. McBride, "A new route to polyselenoethermacrocycles. Catalytic macrocyclization of 3,3-dimethylselenatane by $[Re_2(CO)_9]$", Chem. Commun., Issue 6, pp. 525-526, 1997.

[19] R.D. Adams, K. T. McBride and R.D. Rogers, "A New Route to PolyselenoetherMacrocycles. Catalytic Macrocyclization of 3,3-Dimethylselenetane by $Re_2(CO)_9SeCH_2CMe_2CH_2$", Organometallics, Vol. 16, pp. 3895-3901, 1997.

[20] R. D. Adams, J. L. Perrin, J. A. Queisser and J. B. Wolfe, "Catalytic Macrocyclization of 3,3-Dimethylthietane by $Re_2(CO)_9(SCH_2CMe_2CH_2)$", Organometallics, Vol. 16, pp. 2612-2617, 1997.

[21] D. G. Booth, W. Levason, J. J. Quirk, G. Reid and S. M. Smith, "Synthesis and characterisation of transition-metal complexes involving cyclic diselenoether ligands", J. Chem. Soc. Dalton Trans., Issue 19, pp. 3493-3500, 1997.

[22] T. Kumagai and S. Akabori, "Preparation of Novel Selenacrown Ethers and Their Complexing Abilities with Transition Metal and Heavy Metal Cations", Chem. Lett., Vol. 18, pp. 1667-1670, 1989.

[23] M. K.Davies, M. C. Durrant, W. Levason, G. Reid and R. L. Richards, "Synthesis, spectroscopic and structural studies on transition metal carbonyl complexes of cyclic di- and tetra-selenoether ligands", J. Chem. Soc. Dalton Trans., Issue 7, pp. 1077-1084, 1999.

[24] J. Connolly, M.K. Davies and G. Reid, "Manganese(I) selenoether chemistry: synthesis, multinuclear NMR studies and the structures of $[MnCl(CO)_3(MeSeCH_2CH_2SeMe)]$, $[MnCl(CO)_3(MeSeCH_2CH_2CH_2SeMe)]$ and $[MnBr(CO)_3\{C_6H_4(SeMe)_2\text{-}o\}]$", J. Chem. Soc. Dalton Trans., Issue 22, pp. 3833-3838, 1998.

[25] W. Levason, J. J. Quirk, G. Reid and S. M. Smith, "Synthesis, spectroscopic and redox properties of ruthenium complexes with selenoethermacrocycles: crystal structures of cis-$[RuCl_2([16]aneSe_4)]$ and trans-$[RuCl(PPh_3)([16]aneSe_4)]PF_6$ ($[16]aneSe_4$ = 1,5,9,13-tetraselenacyclohexadecane)", J. Chem. Soc. Dalton Trans., Issue 20, pp. 3719-3725, 1999.

[26] W. Levason, J. J. Quirk and G. Reid, "Synthesis and characterisation of selenoethermacrocyclic complexes of Co^{III}, Rh^{III} and Ir^{III}: crystal structures of trans-$[CoBr_2([16]aneSe_4)]BPh_4$ and trans-$[IrBr_2([16]aneSe_4)]BPh_4$($[16]aneSe_4$= 1,5,9,13-tetraselenacyclohexadecane)", J. Chem. Soc. Dalton Trans., Issue 18, pp. 3713-3719, 1996.

[27] D. J. Gulliver, E. G. Hope, W. Levason, S. G. Murray and G. L. Marshall, "Synthesis, properties, and multinuclear nuclear magnetic resonance (^1H, ^{77}Se, and ^{195}Pt) studies on diselenoether complexes of palladium, platinum, and rhodium", J. Chem. Soc. Dalton Trans., Issue 6, pp. 1265-1269, 1985.

[28] N. R. Champness, W. Levason, J. J. Quirk, G. Reid and C. S. Frampton, "Synthesis, spectroscopic and structural characterization of Pd^{II} and Pt^{II} complexes of the cyclic diselenoether 1,5-diselenacyclooctane, $[8]aneSe_2$", Polyhedron, Vol. 14, pp. 2753-2758, 1995.

[29] W. Levason, J. M. Manning, P. Pawelzyk and G. Reid, "Synthesis and Properties of Organometallic Pt^{II} and Pt^{IV} Complexes with Acyclic Selenoether and Telluroether Ligands and SelenoetherMacrocycles", Eur. J. Inorg. Chem., Issue 21, pp. 4380-4390, 2006.

[30] W. Levason, G. Reid and S. M. Smith, "Chromium(III) complexes of polydentate and macrocyclicselenoethers—synthesis, spectroscopic and exafs studies", Polyhedron, Vol. 16, pp. 4253-4256, 1997.

[31] P. F. Kelly, W. Levason, G. Reid and D. J. Willams, "Selenoethermacrocyclic chemistry: trans-[$RhCl_2$([16]aneSe_4)]BF_4, synthesis, single crystal X-ray structure and ^{77}Se NMR study ([16]aneSe_4= 1,5,9,13-tetraselenacyclohexadecane)", J. Chem. Soc. Chem. Commun., Issue 23, pp. 1716-1718, 1993.

[32] T. -F. Lai and C. -K. Poon, "Crystal and molecular structure of cis-dichloro(1,4,8,11-tetrathiacyclo-tetradecane)ruthenium(II) dihydrate; a correction to the reported stereochemistry based on infrared spectroscopy", J. Chem. Soc. Dalton Trans., Issue 8, pp. 1465-1469, 1982.

[33] M.K. Davies,W. Levason and G. Reid, "Macrocyclicselenoether complexes of nickel(II). Synthesis and properties of [NiX_2([16]aneSe_4)] ([16]aneSe_4 = 1,5,9,13-tetraselenacyclohexadecane, X = Cl, Br or I) and [NiX_2($MeSeCH_2CH_2SeMe$)$_2$]", J. Chem. Soc. Dalton Trans. Issue 13, pp. 2185-2190, 1998.

[34] N. R. Champness, P. F. Kelly, W. Levason, G. Reid, A. M. Z. Slawin, D. J. Williams, "SelenoetherMacrocyclic Chemistry: Syntheses, NMR Studies, Redox Properties, and Single-Crystal Structures of [M([16]aneSe4)](PF_6)$_2$.cntdot.2MeCN (M = Pd, Pt; [16]aneSe4 = 1,5,9,13-Tetraselenacyclohexadecane)", Inorg. Chem., Vol. 34, pp. 651-657, 1995.

[35] R. J. Batchelor, F. W. B. Einstein, I. D. Gay, J. -H. Gu, B. M. Pinto and X. Zhou, "Stereochemical Analysis of Palladium(II) Complexes of the Selenium Coronands 1,5,9,13-Tetraselenacyclohexadecane and 1,5,9,13,17,21-Hexaselenacyclotetracosane", Inorg. Chem., Vol. 35, pp. 3667-3674, 1996.

[36] W. Levason, J. J. Quirk and G. Reid, "SelenoetherMacrocyclic Complexes of Platinum(IV): Synthesis and Spectroscopic Studies on [Pt([16]aneSe4)X_2][PF_6]$_2$, (X = Cl, Br). X-ray Structure of [Pt([16]aneSe4)Cl_2][PF_6]$_2$", Inorg. Chem., Vol. 33, pp. 6120-6122, 1994.

[37] R. J. Batchelor, F. W. B. Einstein, I. D. Gay, J. -H. Gu, B. M. Pinto and X. -M. Zhou, J. Am. Chem. Soc., "An electron transfer reaction of a selenium coronand-copper(II) complex. Formation of the stable 1,5,9,13-tetraselenacyclohexadecane dication", Vol. 112, pp. 3706-3707, 1990.

[38] V.B. Pett Jr., L.L. Diaddario, E.R. Dockal, P.W. Corfield, C. Ceccarelli, M.D. Glick, L. A. Ochrymowycz and D. B. Rorabacher, "Ring size effects on the structure of macrocyclic ligand complexes: copper(II) complexes with 12-16-membered cyclic tetrathia ethers",Inorg. Chem., Vol. 22, pp. 3661-3670, 1983.

[39] R. J. Batchelor, F. W. B. Einstein, I. D. Gay, J. -H. Gu, B. M. Pinto and X. -M. Zhou, "Redox chemistry of the selenium coronand, 1,5,9,13-tetraselenacyclohexadecane, and a mechanistic study of the electron transfer reaction of its Cu(II) complex", Can. J. Chem. Vol. 78, pp. 598-613, 2000.

[40] R. J. Batchelor, F. W. B. Einstein, I. D. Gay, J. -H. Gu and B. M. Pinto, "The syntheses, ^{77}Se CP-MAS solid state NMR spectra and crystal structures of adducts of the selenium coronand, 1,5,9,13-tetraselenacyclohexadecane, with copper(I) trifluoromethanesulfonate and mercury(II) cyanide", J. Organomet. Chem., Vol. 411, pp. 147-157, 1991.

[41] A. J. Barton, N. J. Hill, W. Levason and G. Reid, "Synthesis and Structural Properties of the First MacrocyclicSelenoether Complex of Arsenic(III): A Rare Example of Exo and Endo Coordination in a Single Species", J. Am. Chem. Soc., Vol. 123, pp. 11801-11802, 2001.

[42] N.J. Hill, W. Levason and G. Reid, Inorg. Chem., "Arsenic(III) Halide Complexes with Acyclic and MacrocyclicThio- and SelenoetherColigands: Synthesis and Structural Properties", Vol. 41, pp. 2070-2076, 2002.

[43] A. J. Barton, A. R. J. Genge, W. Levason and G. Reid, "Synthesis and structures of one-dimensional co-ordination polymers derived from bismuth(III) selenoethermacrocyclic complexes, J. Chem. Soc. Dalton Trans. Issue 13, pp. 2163-2166, 2000.

[44] A.J. Barton, N.J. Hill, W. Levason, B. Patel and G. Reid, "Coordination networks derived from antimony(III) halide complexes with thio- and seleno-ether ligation", Chem. Commun., Issue 1, pp. 95-96, 2001.

[45] A.J. Barton, N.J. Hill, W. Levason and G. Reid, "Synthesis and structural studies on polymeric assemblies derived from antimony(III) halide complexes with bi- and tri-dentate and macrocyclicthio- and seleno-etherligands", J. Chem. Soc. Dalton Trans., Issue 10, pp. 1621-1627, 2001.

[46] W. Levason, M. Matthews, R. Patel, G. Reid and M. Webster, "Unusual structural variations within a family of thioethermacrocyclic complexes. Tin(IV) halide adducts of [12]-, [14]- and [16]-aneS_4", New J. Chem. Vol. 27, pp. 1784-1788, 2003.

[47] N. J. Hill, W. Levason, R. Patel, G. Reid and M. Webster, "Unusual structural trends in the [MCl_3([8]aneSe_2)] (M = As, Sb, Bi) adducts", Dalton Trans., Issue 7, pp. 980-981, 2004.

